The quest for secondary structure in chiral dendrimers

Susan E. Gibson* and Jacob T. Rendell

Received (in Cambridge, UK) 17th August 2007, Accepted 1st October 2007
First published as an Advance Article on the web 26th November 2007
DOI: 10.1039/b712298e

This review highlights important developments in the pursuit of chiral conformational order in dendritic structures. To be able to create and control chiral secondary structure necessitates a thorough understanding of how chiral subunits influence the macroscopic structure. Recent studies involve highly sophisticated manipulation of macroscopic chirality through a creative combination of a wide range of synthetic, computational and analytical techniques.

Introduction and background

A fundamental understanding of how individual elements of a large molecular structure can be used to create and control its molecular properties is necessary to underpin the full exploitation of macromolecules and supramolecular structures in applications such as catalysis, drug delivery, molecular recognition, and light emitting and light harvesting processes.[1–5] Dendritic type molecules have for some time been considered good models for disordered and semi-ordered structures such as polymers, aggregates, clusters and liquid crystals, and they are increasingly finding applications of their own. For example, Dendritic Nanotechnologies have recently exploited the voids in polyamidoamine dendrimers to encapsulate cisplatin or carboplatin anticancer drugs for efficient delivery.[6] The dendrimer–drug conjugate is active against aggressive tumour models, is water-soluble and has lower toxicity, and greater stability on storage than the unbound drug.

With respect to chirality, a wide range of dendritic structures has been explored in order to probe the relationship between the chirality of individual elements and the properties of the global structure of the macromolecule.

The aim of this review is to rationalise some of the diverse studies which have been conducted in the last 15 years, and to demonstrate how an increased understanding of the interplay between local and global chirality is starting to lead to greater control of chiral conformational order, thus opening up a plethora of possibilities for applications of these complex macromolecules. Previous reviews in the area of chiral dendrimers have primarily focussed on their synthesis or applications.[7]

The first section of this review will describe studies of dendrimers of disparate structure, which led to the conclusion that chiral secondary structure was present in the macromolecule. Subsequently, a selection of examples will be discussed which highlight how chiroptical studies that indicate the presence of chiral conformational order may be misleading. Finally, a cherry pick of cases will be examined, in which the powerful combination of sophisticated synthetic chemistry and analytical technology has led to a well-documented, comprehensive understanding and control of chiral secondary structures. For greater clarity we provide the reader with brief explanations of the terms used in the assessment of chirality as listed in Table 1.

The search for secondary structure

Several groups have studied the chiroptical behaviour of chiral dendrimers of increasing generations and found that the macroscopic chirality was influenced by individual chiral subunits within the structure. One popular approach has been

Department of Chemistry, Imperial College London, South Kensington Campus, London, UK SW7 2AY. E-mail: s.gibson@imperial.ac.uk

Sue E. Gibson did her first degree in Cambridge and her DPhil in Oxford under the supervision of Professor S. G. Davies. She was then awarded a Royal Society European Fellowship to study at the ETH, Zürich, with Professor Albert Eschenmoser. In 1985, she returned to the UK to a lectureship in organic chemistry at the University of Warwick and in 1990 she was appointed to a lectureship at Imperial College, London. In 1999, she took up the Daniell Chair of Chemistry at King's College London, returning to Imperial College London and a Chair of Chemistry in 2003. Her research interests lie in the area of the application of transition metals in organic synthesis. Current projects include the development of new catalysts of the Pauson–Khand reaction, the synthesis and applications of novel chiral macrocycles, and the use of chiral-base chemistry and tricarbonylchromium(0) complexes of arenes in the design of new asymmetric catalysts and nanostructures, with a particular emphasis on C_3 *symmetry.*

Jacob Rendell obtained his MChem degree in Chemistry from UMIST (now part of the University of Manchester) in 2004. During his undergraduate studies he spent a year on an industrial placement with GSK in Stevenage (UK), working on the synthesis of anti-hepatitis C agents. He then returned to UMIST, where his final year project focussed on asymmetric aza-Diels–Alder reactions for the synthesis of chiral piperidines under the supervision of Prof. Pat Bailey. Since October 2004 he has been carrying out his PhD research in the laboratory of Prof. Sue Gibson at Imperial College, working on chiral dendrimers and chiral pincer complexes, which are prepared using a chiral base-mediated approach to install multiple stereocentres around (arene)tricarbonylchromium(0) complexes in a single operation.

Table 1 Terms and definitions

Term	Symbol/abbreviation	Definition
Optical rotation (optical activity)	α	The rotation of linearly polarised light as it travels through certain non-racemic materials.
Specific rotation	$[\alpha]$	The observed angle of optical rotation α when plane-polarised light of wavelength λ is passed through a sample with a path length (l) of 1 dm and a sample concentration (c) of 1 g mL^{-1} at temperature T. $$[\alpha]_{\lambda}^{T} = \frac{100\alpha}{lc}$$
Molar rotation	$[\Phi]$	$[\alpha]$/molecular weight (sometimes represented as $[\alpha]_{mol}$ in the literature, but for consistency $[\Phi]$ will be used throughout this review).
Molar rotation/chiral unit	$[\Phi]/n$	The value of molar rotation divided by the number of chiral units in the molecule.
Circular dichroism	CD	A form of spectroscopy based on the differential absorption ($\Delta\varepsilon$) of left- and right-handed circularly polarised light in non-racemic molecules.
Optical rotatory dispersion	ORD	The variation in the specific rotation of a substance with a change in the wavelength of light. May be used to determine the absolute configuration of metal complexes, for example.
Hypochromic effect		A decrease in absorption intensity.
Cotton effect	CE	The characteristic change in ORD and/or CD in the vicinity of an absorption band of a substance. In a wavelength region where the light is absorbed, the absolute magnitude of the rotation at first varies rapidly with wavelength, crosses zero at absorption maxima and then again varies rapidly with wavelength but in the opposite direction. This phenomenon is known as the CE.

to add successive generations of achiral branches to a chiral core, and then to relate the specific and molar rotation to the size of the dendrimer. If a non-linear relationship was observed between optical activity and increasing size, this could imply that the chirality was transmitted from the core through the branches, forcing them to adopt a chiral conformation. Many research groups have made observations of this type but have been unable to fully rationalise the proposed induced chiral conformational order. In elucidating the overall macroscopic chiral conformation of dendrimers, circular dichroism (CD) spectroscopy has proven to be a powerful tool.

In a typical example, Vögtle and co-workers prepared two series of dendritic alkaloid derivatives by attaching achiral polybenzyl ether (Fréchet) dendrons of increasing generations, G, ($G_0 \rightarrow G_3$) to a chiral atropine or quinine core, as exemplified by the second-generation dendrimers **1** and **2** (Fig. 1).[8] The specific rotation showed decreasing values with increasing size of the Fréchet dendrons. In contrast, the magnitude of the CD signal increased for both series as the size of the dendritic substituent increased. (The increase was noted in the 215–220 nm region of the spectrum for the atropine derivatives and 220–230 nm region for the quinine

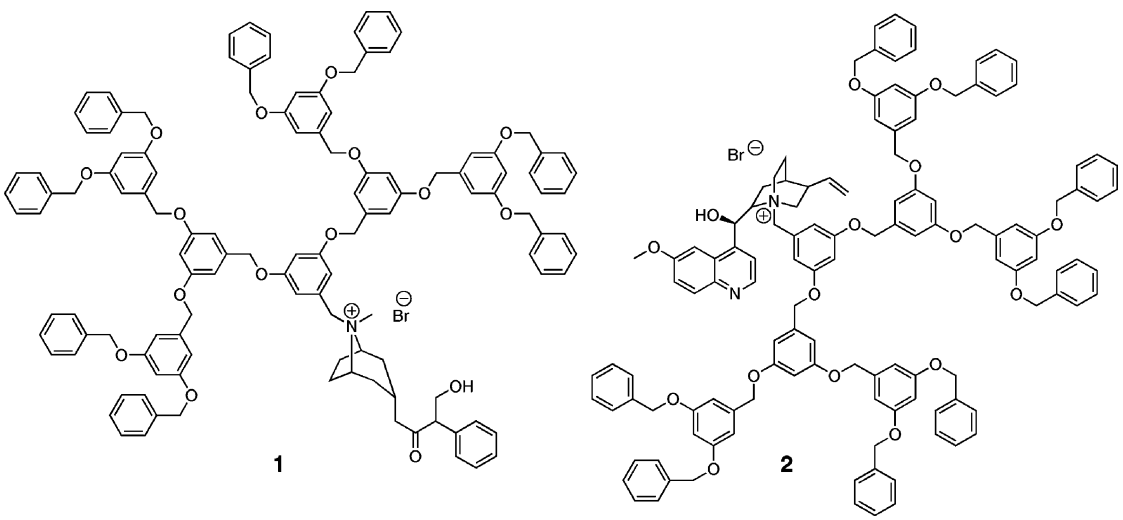

Fig. 1 Second-generation dendronized atropine and quinine.

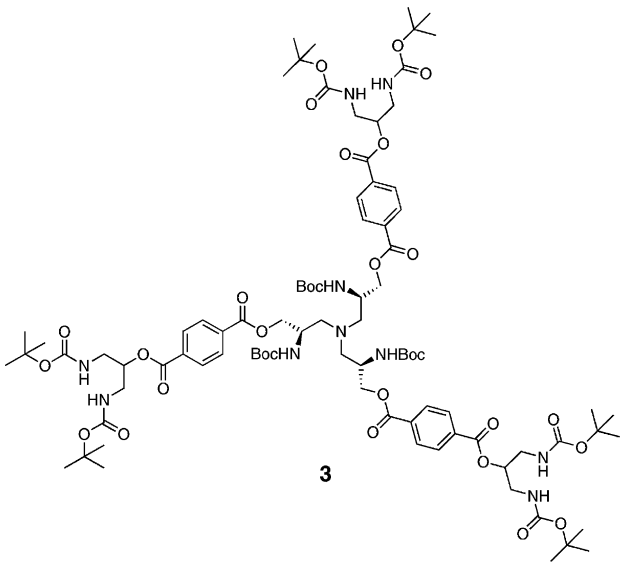

Fig. 2 A first-generation dendrimer containing a chiral tris(2-amino-3-hydroxypropyl)amine core.

analogues.) The authors speculated that the observed CD could be due to a chirally induced formation of a propeller-like arrangement of the benzene rings within the Fréchet dendrons.

A different study of chirality transmission from an optically active core to achiral branches was reported by Hayes and co-workers, who described the synthesis and properties of certain C_3-symmetric chiral dendrimers ($G_0 \rightarrow G_2$).[9] Both enantiomeric series [(*R*,*R*,*R*) and (*S*,*S*,*S*)] were assembled from a chiral tris(2-amino-3-hydroxypropyl)amine core and carbamate terminated dendrons. The first-generation (*S*,*S*,*S*) dendrimer **3** is illustrated in Fig. 2. Whereas the specific rotation [α] decreased with greater branch size, an observation attributed to the decreasing number of stereogenic centres per gram of sample (recall that concentration, *c*, is measured in g mL^{-1} for specific rotation), the molar rotation [ϕ] ([α]/molecular weight) was almost twice as high for G_2-dendrimers compared to G_0 or G_1. This suggested the presence of chiral substructures within the dendritic macromolecule induced by the chiral core. Attempts to probe the overall secondary structure using CD spectroscopy, however, failed to provide further information.

In an unorthodox approach to creating a chiral core, Meijer and co-workers have described a dendrimer which has a core rendered chiral by dendrons of differing generations.[10] Dendrimer (*S*)-**4** and its enantiomer (*R*)-**4** were prepared from a triol core and Fréchet dendrons of varying sizes (Fig. 3). Remarkably, no optical activity could be observed for either (*S*)-**4** or its enantiomer (*R*)-**4** in solution, despite attempted measurements of [α], CD and ORD. Optical activity of the synthetic intermediates was closely monitored in the preparation of **4**, but no racemization was evident. [(*S*)-**4**: $[\alpha]_D = 0.00 \pm 0.01^\circ$; precursor alcohol: $[\alpha]_D = +9.6^\circ$] The authors concluded that the conformational flexibility in (*S*)-**4** would lead to a vanishing enantiomeric difference in the geometry. It was anticipated, however, that higher generation analogues would contain more densely packed surfaces, which would "freeze in a mesoscopic chiral object".

The same research group studied the effect of backfolding dendritic wedges on conformational rigidity (in an attempt to gain further understanding of the influence of structural rigidity upon optical activity).[11] Chiroptical studies of backfolding dendrimers, exemplified by structure **5** in Fig. 4 (a conformationally more rigid analogue of **4**), were conducted, and revealed an $[\alpha]_D$ of $+0.8^\circ$ and a weak CD signal at $\lambda =$ 280 nm at a temperature of 15 °C. At higher temperatures (30 °C), however, this signal disappeared, indicating that the degree of conformational flexibility or rigidity was temperature dependent.

In the pursuit of an understanding of how individual chiral subunits could affect the overall macroscopic chirality of dendrimers, several studies have focussed on the assembly of dendritic structures containing chiral building blocks in both the central unit and the branches. By controlling the chirality of each individual subunit and/or branching point it was anticipated that it would be possible to predict and exert total control over the secondary structure. Seebach and co-workers described the synthesis and associated chiroptical properties of fully chiral dendrimers of the zero to third-generation containing the core **6** and the doubly and triply branched building

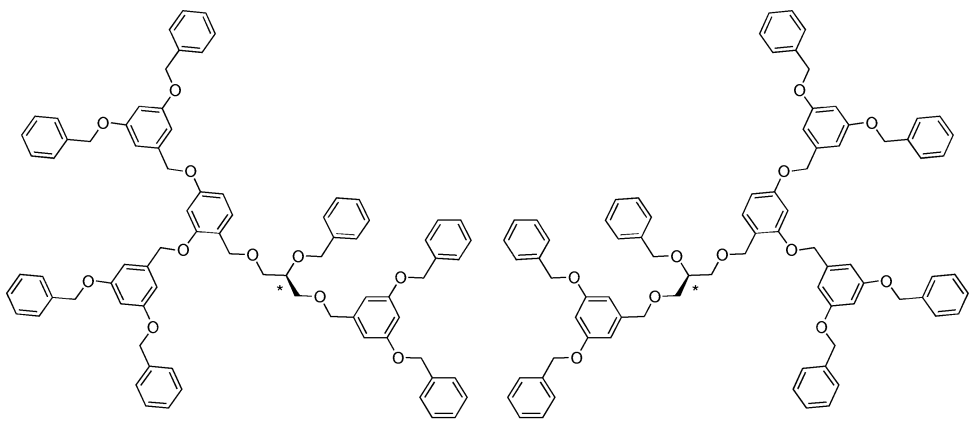

Fig. 3 Cryptochiral dendrimers.

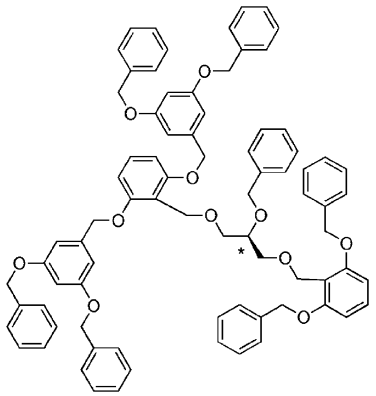

5

Fig. 4 A chiral dendrimer with backfolding wedges.

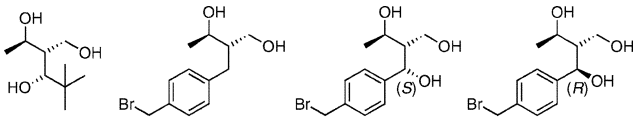

6 **7** **8** **9**

Fig. 5 Chiral core **6** and doubly and triply branched chiral building blocks **7–9**.

blocks **7–9** illustrated in Fig. 5.[12,13] It was reported that the sign of specific rotation was reversed on going from the first- to the second-generation for triply branched dendrimers, such as the second-generation macromolecule **10** in Fig. 6 [containing chiral core **6** and two layers of (*S*)-configured building block **8**].[12] Similarly the sign and amplitude of the CD signal was variable in the region of 220–240 nm and changed from generation to generation, in particular on going from the

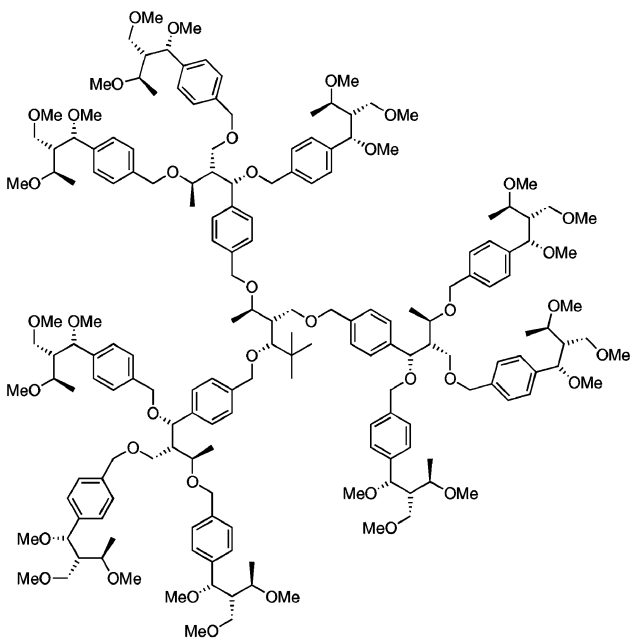

10

Fig. 6 A triply branched chiral dendrimer containing stereogenic centres at each branching point.

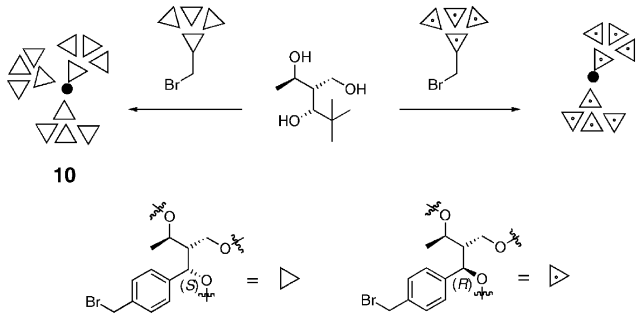

Scheme 1 Diastereoselective assembly of chiral core and building blocks.

second to the third. The authors suggested that this "may be an indication of conformationally chiral substructures in the dendrimer branches". Interestingly, during the preparation of the triply branched second-generation dendrimer, the authors noted that the triply branched macromolecule **10** was formed if the (*S*)-configured building block was used, but that only a doubly branched dendrimer was formed if the corresponding (*R*)-building block was employed (Scheme 1).

In a later paper by Seebach and co-workers,[13] it is of note that the authors commented upon the challenges associated with interpretation of chiroptical properties in dendritic systems, as the individual chiral building blocks of different layers reside in different environments.

In order to probe the quantitative relationship between the optical rotation properties and the number of chiral units, as well as their specific location within the structure, Chow *et al.* prepared a series of homochiral[14,15] and heterochiral layered tartrate-derived dendrimers, of which two are shown in Fig. 7. The chiroptical properties of the homochiral dendrimer **11** were compared with two heterochiral partners: one with three (D)-chirons in the inner layer and six (L)-chirons in the outer layer (**12**), and one with three (D)-chiral units in the inner shell, and three (D)- and three (L)-chiral units in the outer shell (not depicted).[16,17]

The molar rotation was found to be proportional to the number of tartrate units and the chiroptical effects of an (L)-tartrate derived unit cancelled out that of a (D)-tartrate on a 1 : 1 basis, irrespective of their positions within the macromolecule. Consequently, the overall molar rotation of a dendritic section was proportional to the number of (L)- or (D)-chirons in excess. The average contribution per (D)-tartrate unit towards molar rotation was $+145^{\circ}$, which was slightly less than the (L)-tartrate (-185°). CD studies revealed that the homochiral dendrimer **11** gave two strong negative Cotton effects (CE) at 200 and 210 nm whereas in **12** the positive CE at 210 nm was less prominent, suggesting a reduced cooperativity between the units of the heterochiral system compared to the homochiral.

Recently, we reported an exploration of diastereoisomerism within small C_3-symmetric dendritic structures.[18] Comprehensive circular dichroism studies revealed a dramatic difference (>10 fold) in amplitude of the CD signal in the near-UV region (240–280 nm) for homochiral dendrimer ($S_{inner}S_{outer}$)-**13** (and its enantiomer) compared with the heterochiral dendrimer ($R_{inner}S_{outer}$)-**13** (and its antipode), illustrated in Fig. 8.

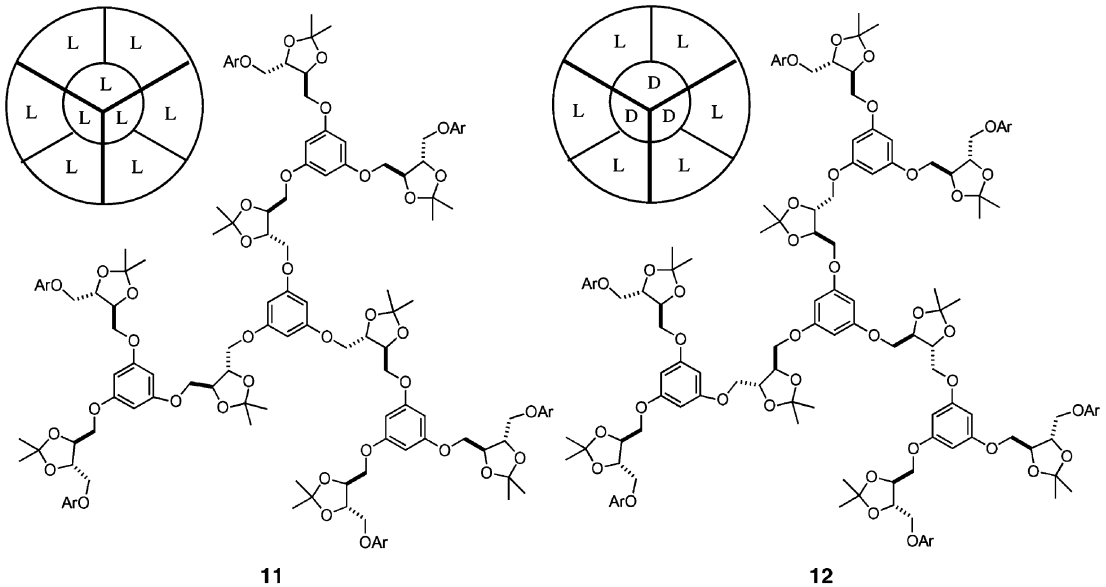

Fig. 7 Homo- and heterochiral dendrimers derived from tartaric acid.

We proposed that in the heterochiral system the aryl groups act as rotating paddles about the long axis (Fig. 9), whereas in the homochiral system the rotation is restricted, leading to a stronger ^1L_b transition along the long axis (of the peripheral phenyl rings) and thus a greater amplitude of the CD signal.

Another study of diastereoisomeric dendrimers was reported by Lellek and Stibor,[19] who examined the structural features of homochiral isomer **14a** (Fig. 10), based on (*R*)-2,2′-dimethoxy-1,1′-binaphthalene building blocks, and its heterochiral partner **14b**. The CD measurements revealed a pronounced hypochromic effect (mainly observed for homochiral dendrimer **14a**) and also showed good agreement between calculated and observed $\Delta\varepsilon$. It was proposed that the observed hypochromic effect was caused by dynamic intramolecular interactions. This hypothesis was substantiated by a detailed NMR study, which indicated the presence of hydrogen bonding between the amide protons and the methoxy oxygens in the dendritic molecule. Moreover, the NMR study showed that the homochiral dendrimer **14a** could slowly interconvert and adopt several conformations. Notably, this hydrogen bonding was broken and the NMR spectra of **14a** and **14b** became almost identical when DMSO-d_6 was used as the solvent instead of $CDCl_3$. The authors concluded that the hypochromic effect observed for the homochiral dendrimers was caused by conformational flexibility and internal organisation of the chains inside the molecules, and that the diastereomeric pair exhibited different types of conformational behaviour. Interestingly, chiroptical measurements suggested that the molar rotation was linearly related to the number of monomer building blocks and was comparable to theoretical values. Thus, in this particular case, measurement of molar rotations alone would not have revealed conformational behaviour and internal organisation.

Studies have also been undertaken on dendrimers with chirality placed only at the periphery. For example, Meijer and co-workers reported a series of poly(propylene imine) dendrimers of first to fifth generation which were decorated with a range of Boc protected (L)-amino acids or (D)-phenylalanine, leading to congested macromolecules with 4, 8, 16, 32 or 64 end groups.[20] The optical activity of these increasingly

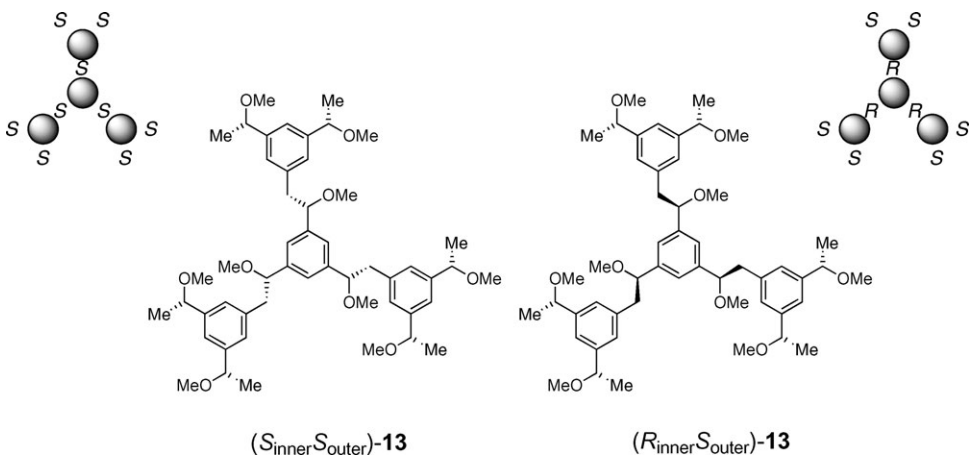

Fig. 8 Homo- and heterochiral polyether dendrimers.

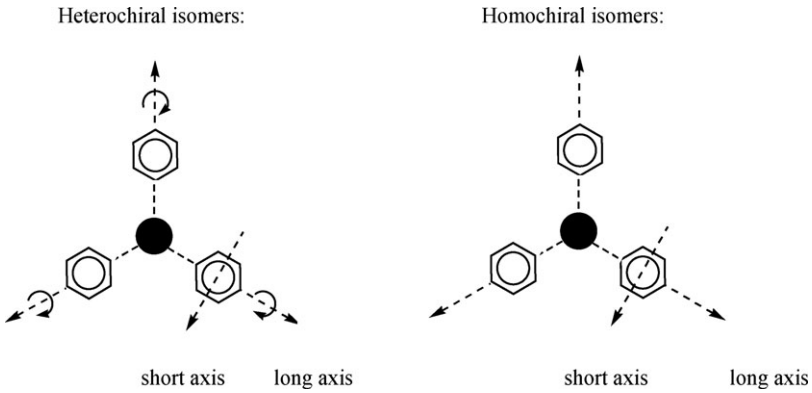

Fig. 9 The aryl groups are free to rotate about their long axes in the heterochiral isomers, while the rotation is restricted in the homochiral isomers.

crowded chiral surfaces was studied in some detail, in order to determine the packing properties of the peripheral amino acids and to evaluate the potential use of these macromolecules as encapsulating dendritic "boxes" in host–guest chemistry. A dramatic decrease in [α] was observed with increasing dendrimer generation for all amino acid derived macromolecular systems studied. CD spectroscopy of the (D)-Phe and (L)-Phe dendrimer series revealed that the CD signal decreased in magnitude with higher generations in the 235–270 nm region of the spectrum. A decrease in the Cotton effect was accompanied by a small change in the associated UV spectra, which the authors claimed was indicative of a change in conformation. Similar chiroptical effects were observed for dendrimers carrying different amino acids at the periphery. It was suggested that the dense packing of the peripheral groups in these highly organised dendritic structures induced the amino acids to adopt two pseudo-enantiomeric conformations that align themselves in such a way that they diminish the chiroptical properties.

It is perhaps pertinent at this point to compare the dendrimer-based studies described above with related studies on polymers, and, in particular with a study of a polymer decorated with dendrimers. In a recent publication, Masuda and co-workers reported the synthesis and a conformational study of the poly(phenylacetylene) **15** (Fig. 11), bearing an (L)-lysine based dendritic side chain.[21] The conformation of polymer **15** was examined by CD spectroscopy, which revealed that the macromolecule adopted a helical conformation with

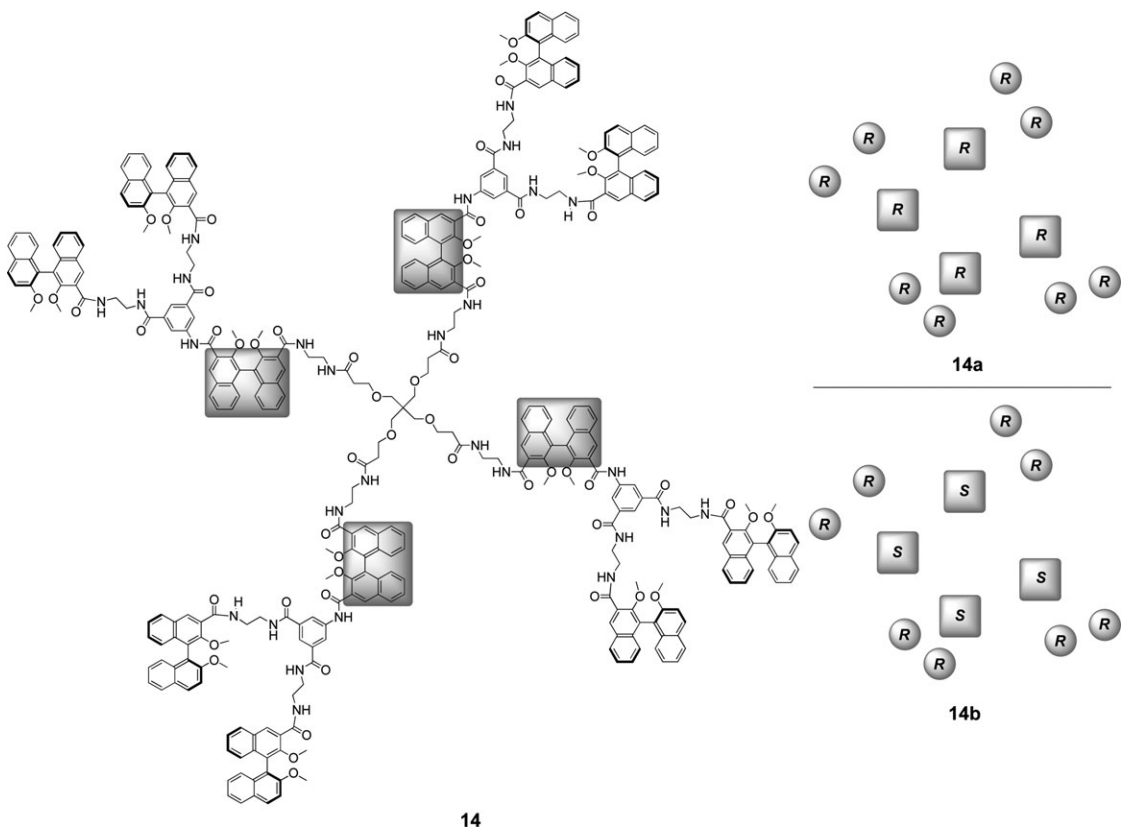

Fig. 10 Homo- and heterochiral dendrimers with axially chiral units.

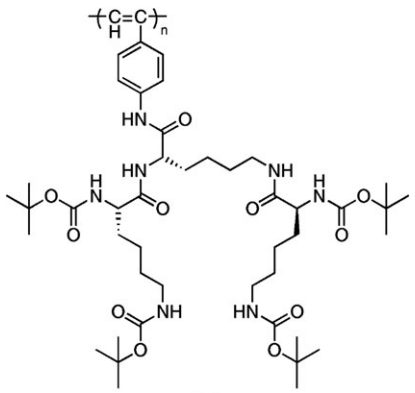

15

Fig. 11 (L)-Lysine dendronized poly(phenylacetylene).

predominantly a one-handed screw sense in THF or $CHCl_3$ or in a film state, whereas in MeOH this conformation was much harder to recognise in the 250–450 nm region of the CD spectrum. It was found that the one-handedness of **15** in a $CHCl_3$ solution decreased with increasing temperature, or on addition of a protic solvent. In contrast, the helix was stable to changes in temperature in THF. Solution and solid-state IR spectroscopy confirmed that the helical structure was stabilised by intramolecular hydrogen bonding between the amide and carbamate groups in the side chains.

Cases of mistaken identity

Non-linear behaviour of chiroptical data has frequently been used as a preliminary indication that macromolecules adopt some form of chiral conformational order. Further examination, however, sometimes reveals 'cases of mistaken identity', whereby certain structural features, constitutional changes, or solvent effects have influenced the optical properties of the dendrimers, thus complicating the elucidation of their chiral architecture.

Careful analysis of optical data is important in the search for secondary structure as indicated in some of the studies already described, and in the following elegant study of Majoral and co-workers, who examined how a progressive burying of chiral ferrocene derivatives affected the electrochemical and chiroptical properties of dendrimers.[22] The chiral units were placed precisely on one individual shell within the dendritic skeleton (for example on shell 3 as illustrated in Fig. 12) and then buried under further layers in order to determine whether the location of the chiral ferrocene would affect the chiroptical or electrochemical behaviour of the macromolecule. The latter proved to be dependent on how deeply the ferrocene was buried, reflecting the ease of electron transfer between the external electrode and the redox centres. With respect to chiroptical properties, the specific rotation was directly related to the degree of burial of the chiral shell and not to its distance from the dendrimer core. For example in dendrimers G_{3+1}, G_{5+1} and G_{9+1} the specific rotation [α] was found to be $+408.6 \pm 6.5^\circ$ (entries 1–3, Table 2), whilst in G_{3+2}, G_{5+2} and G_{9+2} the [α] was measured to be $+233.5 \pm 2.5^\circ$ (entries 4–6, Table 2). Further analysis, however, revealed that the molar rotation [ϕ] only depended on the number of chiral groups present, suggesting that the relative burying of the stereogenic units inside the dendrimer had no influence upon its chiroptical properties.

In several reported cases, a structural change in the dendritic core was found to be responsible for chiroptical effects, rather than induced chiral secondary structure. For example, Vögtle and co-workers described the synthesis and associated CD

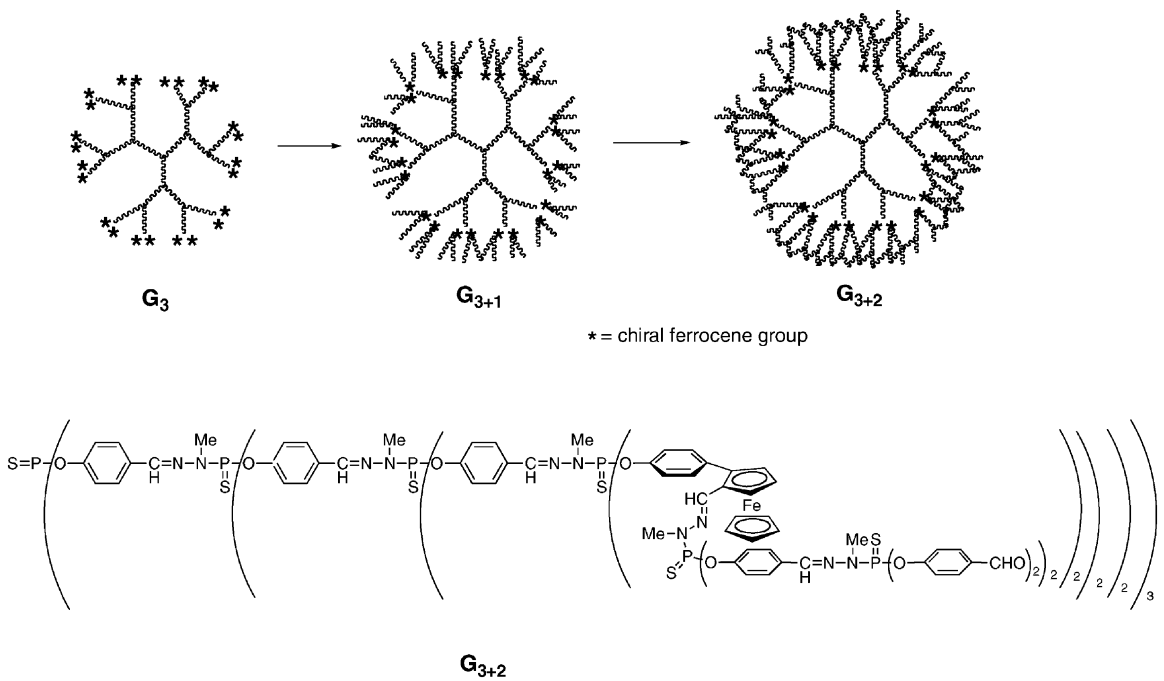

Fig. 12 Controlled 'burial' of chiral ferrocene groups affected electrochemical properties of dendrimers G, but no evidence was obtained for the creation of chiral secondary structure.

Table 2 Chiroptical data for chiral ferrocene containing dendrimers G_{x+y}

Entry	Dendrimer	[α]	[ϕ]/chiral units
1	G_{3+1}	+415.1	342
2	G_{5+1}	+404.3	341
3	G_{9+1}	+402.1	341
4	G_{3+2}	+236.1	352
5	G_{5+2}	+232.2	350
6	G_{9+2}	+231.0	349

spectra of generations of Fréchet dendrons emanating from a paracyclophane, rotaxane or catenane core.[23] In the study of enantiomeric dendrorotaxanes with dendrons attached to both the axle and the wheel (see for example the second-generation dendrimer **16**, Fig. 13), a slight shift of the CD band from 216 to 181 nm was observed with increasing generations, indicative of conformational changes in the structure of the chiral core. The authors rationalised this by proposing that an increase in dendron size would cause the wheel of the rotaxane to change position on its axle.

Similarly, dendrimers with optically active binaphthol groups at their core have been studied and their chiroptical properties have been found to be dominated by the binaphthol core. Chen *et al.*[24] and Meijer and Peerlings[25] investigated this class of dendrimers (Fig. 14) independently and concurrently in 1998. They both established that the dihedral angle between the naphthyl units of the core increased with higher generation due to a greater steric repulsion between the dendritic branches. This was manifested in a concomitant increase in CD magnitude. In addition, Meijer and Peerlings observed that an increase in size of the Fréchet dendrons led to a more negative value for the molar optical rotation, which was also attributed to the change in the torsional angle of the core.

Later Meijer and co-workers attempted to establish a quantitative correlation between changes in the magnitude of the CD signal ($\Delta\varepsilon$) and the dihedral angle θ.[26] More specifically the CD signal corresponding to the exciton couplet in the

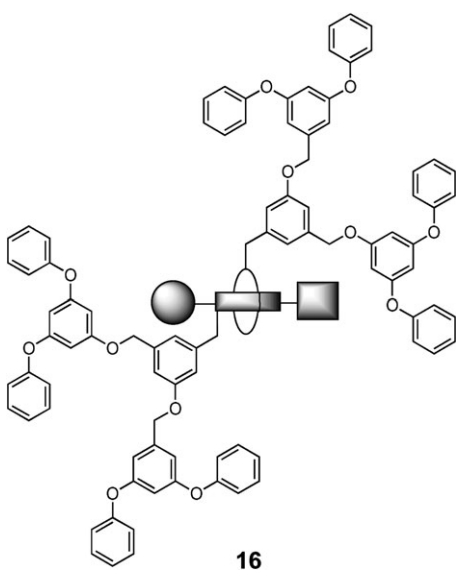

Fig. 13 A second-generation dendro[2]rotaxane.

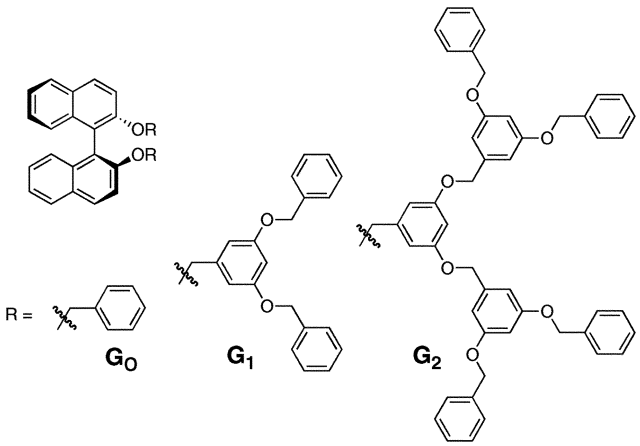

Fig. 14 Dendrimers with axially chiral core.

^{1}B spectral region (*ca.* 230 nm) of the 2-naphthol chromophore was investigated.

The results from the study were classified into four categories according to the magnitude of the CD signal in relation to the size of the dihedral angle (Table 3). It was noted that for the (*S*)-binaphthol derivatives the sign of the CD signal was positive for $0 < \theta < 110^\circ$ and negative for $110 < \theta < 180^\circ$. Moreover the dihedral angle never exceeded the critical value of 110°. The magnitude of the CD signal was plotted against dihedral angle and the authors observed that the experimental values were in agreement with the values obtained from MMX calculations. The greatest steric bulk, induced by the back-folding dendrons (Class D, Table 3) gave rise to the largest dihedral angle (even bigger than the angle induced by G_3 or G_4 dendrons from Class C) and the smallest intensity of the CD signal. This study demonstrated the value of CD spectroscopy as an analytical tool for obtaining structural information about dendrimers.

Table 3 Modified binaphthols and their associated dihedral angles θ

Class	$\Delta\varepsilon$	θ/°	R	
B	300–350	60–75		n = 1–4
A	200	90	Me, Bn	
C	100–140	95–100	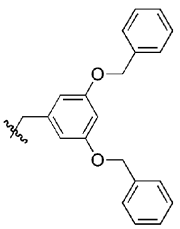	G_2,G_3,G_4
D	40–60	104, 107	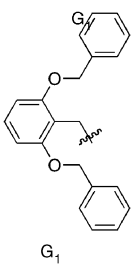	G_2

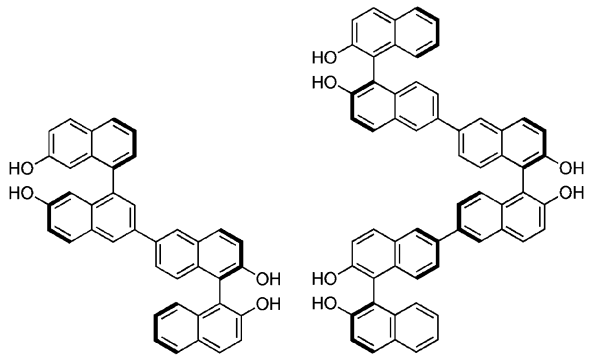

17 18

Fig. 15 (*R*,*R*)-Tetranaphthyl and (*R*,*R*,*R*)-hexanaphthyl chiral cores.

Lin and co-workers also conducted a study of dendrimers containing a chiral binaphthyl core and the extended chiral oligomeric binaphthyl cores **17** and **18** (Fig. 15), decorated with Fréchet dendrons, and reported their photophysical and chiroptical properties.[27] Similar to Meijer's observations (*vide supra*) it was found that the dihedral angle associated with the 1,1′-linkages between the naphthyl rings increased with greater steric bulk/higher generations of the dendrons. In addition CD spectroscopy revealed that the Cotton effects of the dendrimers were the same as their corresponding chiral cores, indicating that the absolute configuration of the macromolecules was maintained on addition of the achiral dendrons to the chiral core. The authors also demonstrated that the fluorescence intensity increased with higher generations for most of the chiral dendrimers, consistent with the greater number of fluorophores. It was noted, however, that the chiroptical data suggested that no chirality transfer was taking place in this dendritic system. Lin and co-workers proposed that this could be due to lack of conformational rigidity in the branches.

In an attempt to study energy transfer in an optically pure dendritic system, Pu *et al*. examined a series of structurally rigid dendrimers containing a chiral binaphthol core and phenylacetylene dendrons of increasing generations, exemplified by the zero-generation dendrimer **19** (Fig. 16). The long-

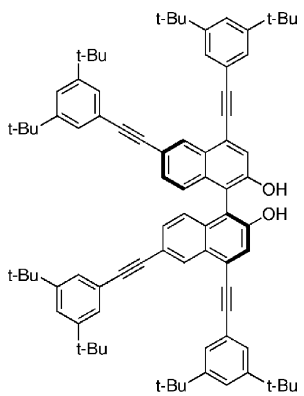

19

Fig. 16 A zero-generation dendrimer with phenylacetylene dendrons attached to a chiral binaphthyl core.

term goal of this project was to develop an enantioselective fluorescence sensor.[28] Following collection of the optical rotation data, it was found that there was only a 36% increase in the molar rotation between the zero- and second-generation dendrimer. It was concluded that the phenylacetylene branches did not lead to major chiral amplification throughout the rigid dendritic structure. Moreover, on examining the CD spectra of these dendrimers, the authors found that no significant change in the Cotton effect was occurring on going from G_0 to G_2. This observation also demonstrated that there was no significant chiral amplification, and that no chiral order was achieved by the dendritic branches. Notably, the strong emissions in the fluorescence spectra of the dendrimers at >420 nm were indicative of a highly efficient intra-molecular energy transfer from the phenylacetylene branches to the more conjugated core, a phenomenon which was further supported by the measurement of the excitation spectra. Thus the energy harvested by the periphery on irradiation could be efficiently transferred to the dendritic core.

As the number of phenylacetylene chromophores increased, more photons could be harvested by the higher-generation dendrimers. The authors pointed out that the observed increase in fluorescence quantum yield for the higher-generation dendrimers could have been caused by hindered rotation around the 1,1′-binaphthyl bond as the size of the dendrons increased.

In a later communication, Pu described the chiroptical and fluorescence properties of a series of related chiral dendrimers containing a binaphthyl core and achiral phenylene-based branches.[29] Similar observations were made with respect to the efficiency of energy migration from the branches to the core, as reported previously (*vide supra*), but again no macroscopic chiral order could be defined.

Several studies have recognised the possibility that slight changes in the constitution of chiral units may have a significant effect on chiroptical data. A typical example is the investigation by Ritzén and Frejd of the chiroptical properties of two complementary types of decongested chiral polypeptide dendrimers, such as G_1 dendrimers **20** and **21** (Fig. 17).[30] Chirality was introduced during the synthesis of the corresponding monomers, $\mathbf{20}_{\text{monomer}}$ and $\mathbf{21}_{\text{monomer}}$, by means of asymmetric hydrogenation. A study of the relationship between the chiroptical parameters of the individual monomers and the whole macromolecule was conducted in order to detect whether or not secondary structure was present in the dendrimers. The CD spectra of the second-generation dendrimers were compared with those of their corresponding monomeric constituents. Excellent agreement between observed and calculated CD spectra suggested that these two particular dendrimers adopted a flat, spread-out shape in THF solution with minimal steric packing. In contrast $[\phi]_D$/chiral unit appeared to decrease with increasing size of the dendritic structures. The authors suggested that this could be due to constitutional differences between the structures.

Constitutional effects have been studied meticulously by McElhanon and McGrath, who warned how they could be mistaken for induced chiral secondary structure.[31] A series of dendrimers G_0–G_2 were synthesised from the core molecule **22** and chiral monomeric subunits **23**, **24** or **25** (Fig. 18), and the

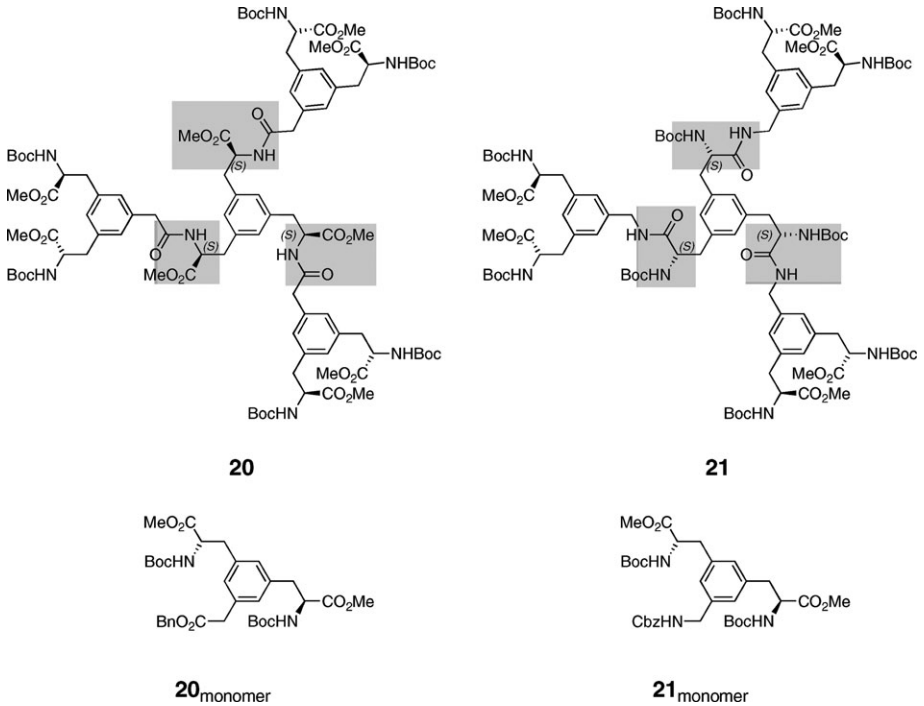

Fig. 17 First-generation polypeptide dendrimers and their corresponding monomers.

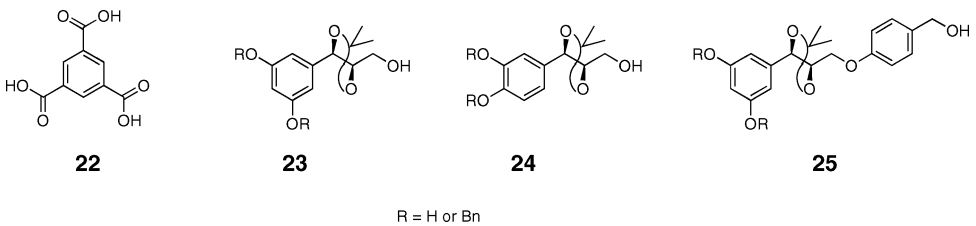

Fig. 18 Dendritic core and three types of chiral monomeric subunits. (Note that G_0 dendrimer contains three monomeric subunits; G_1 contains nine monomeric subunits *etc*.)

role that the molecular constitution played in the variation in molar rotation values was investigated.

From the chiroptical data presented in Table 4, it was revealed that the value for molar rotation/chiral unit, $[\Phi]/n$, changed significantly as the dendrimer generation increased for dendrimers containing chiral subunits **23** and **24** (entries 1–6, Table 4), but not for dendrimers containing chiral subunit **25** (entries 7–9). The authors initially suggested that this could be a possible indication of chiral conformational order in the former two series of dendrimers, where closer packing of subunits would lead to better intramolecular communication. CD spectroscopy indicated an increase in signal intensity in the 200–240 nm region of the spectrum on increasing dendrimer size for the series that contained monomer **23**. The optical activities of lower molecular weight model compounds **26** ($[\phi]_D = +262^\circ$) and **27** ($[\phi]_D = +122^\circ$), prepared to simulate different regions of dendrimer **28** (Fig. 19) and higher-generation analogues, implied that as the generation size increased slight constitutional changes may have a strong effect on the chiroptical properties of the dendrimers. The authors calculated $[\phi]$ values for a range of dendrimers with differing constitution and generation size, using the $[\phi]$ values for **26**, **27** and other low molecular weight compounds, and found that these agreed within 14% of the observed values for the macromolecules.

Table 4 Molar rotation data for chiral dendrimers G_0–G_2 containing monomeric units **23**, **24** or **25**

Entry	Monomer	Generation (x)	$[\Phi]/^\circ$	$([\Phi]/n)/^\circ$
1	**23**	0	+356	+119
2		1	+2204	+245
3		2	+5948	+283
4	**24**	0	+372	+124
5		1	+2232	+248
6		2	+6039	+288
7	**25**	0	+1598	+533
8		1	+4992	+555
9		2	+11 172	+532

Later, McElhanon and McGrath carried out further studies of constitutional effects upon chiroptical properties in dendritic structures.[32] As the acetonide-protecting groups in structures **23–25** (see Fig. 18) restricted rotation about the bond containing the two stereogenic centres and rendered the conformation of the subunits relatively invariable, the authors prepared a range of constitutionally different chiral dendrimers containing subunits with greater

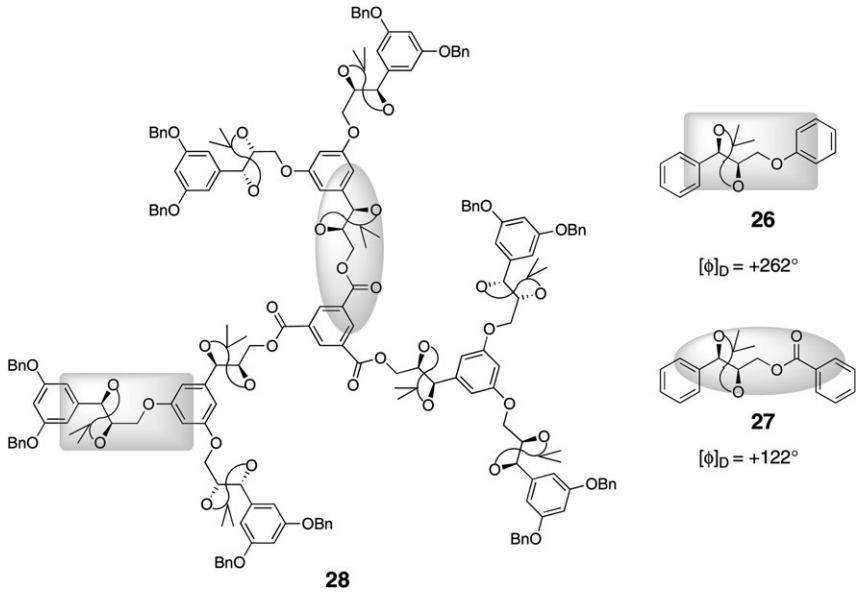

Fig. 19 First-generation chiral dendrimer **28** and corresponding low-molecular weight model compounds (**26** and **27**).

conformational flexibility, as illustrated by the 3,5-disubstituted zero-generation chiral dendrimer **29** and the 3,4-disubstituted dendrimer **30** (Fig. 20). Inspection of $[\phi]/n$ revealed a constant value for the G_0 structures **29** and **30**, but a significant increase as dendrimer generation increases from G_0 to G_1 for the 3,5-disubstituted dendrimer. As the optical activity of the dendrimers compared well with values calculated using data derived from carefully selected model fragments (within 4.5%), chiral conformational order was not evident. Instead, the authors again concluded that the observed discrepancies in molar rotation with increasing dendrimer generation were a result of constitutional effects.

Junge and McGrath also reported the synthesis and chiroptical studies of chiral dendrons, which contained a chiral hydrobenzoin-derived subunit **31** that had been placed in individual generational shells at increasing distance from the focal point of the dendron, as depicted in Fig. 21.[33] It was proposed that the isolation of chiral units at different positions within the dendritic structure would allow the study of the effect of subunit position on dendrimer conformation. The molar rotation per chiral subunit based on alcohol **32** (Fig. 22) was found to increase as the chiral unit proceeded from the focal point (first-generation dendron **33**) to shells further into the interior of the dendritic structure (second- to fourth-generation dendrons **34–36**). At first sight, the chiral subunit **31** appeared to have a larger effect on the optical rotatory power when it was buried in the dendritic structure, indicating conformational order in dendrons **34–36**. By using the specific rotation of chiral model unit **37** (Fig. 22) to analyse the dendrons, however, the authors concluded that the observed difference in $[\Phi]/n$ values between first shell chiral dendron **33** and **34–36** was based exclusively on constitutional changes and not on conformational order in the dendritic structure.

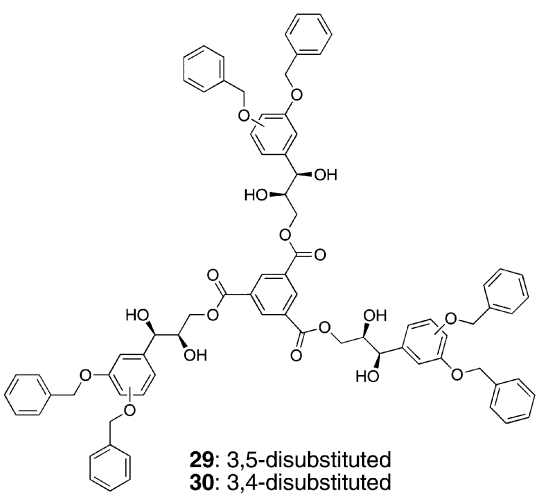

Fig. 20 Chiral dendrimers with different constitution.

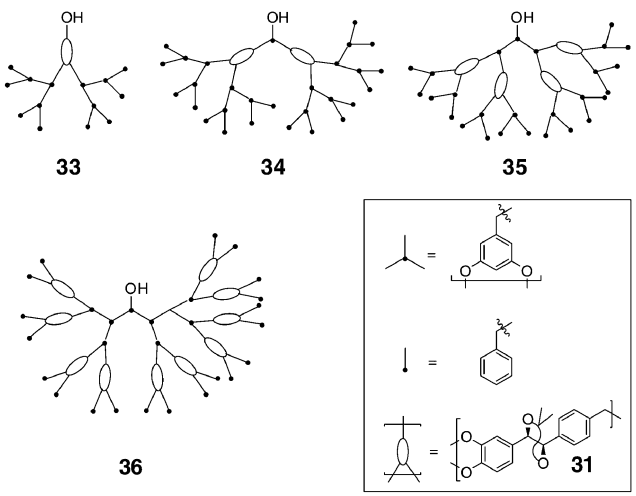

Fig. 21 Chiral shell dendrons, G_1 to G_4 (**33–36**), containing a chiral hydrobenzoin-derived subunit **31**.

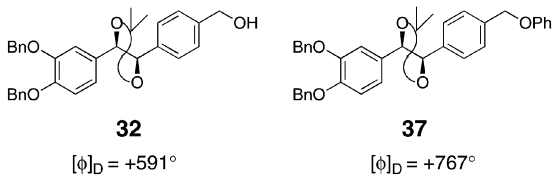

Fig. 22 Two model chiral subunits with their associated molar rotation values.

Solvent effects have been found to influence chiroptical properties. Parquette and co-workers studied the chiroptical properties of successive generations of chiral dendrimers containing ester terminated Fréchet dendrons attached to a chiral core **38**, as illustrated by the first-generation methyl ester terminated dendrimer **39a** in Fig. 23.[34] A decrease in both the specific [α] and molar [ϕ] rotation was observed on going from the first to the third generation. The authors suggested that the decrease in [ϕ] with increasing dendrimer generation could be due, in part, to the increase in steric congestion developing around the central chiral core as the dendritic branches grew in size. Interestingly, the optical rotations were significantly diminished when changing the solvent from $CHCl_3$ to a 1 : 4 THF–MeCN mixture. Parquette and co-workers speculated that the Fréchet dendrons could collapse upon the core in poor solvent systems, leading to a lower optical activity.

A study of chiral amphiphilic dendrimers, such as the carboxylic acid terminated dendrimer **39b** (Fig. 23) and the first-generation (D)-mannitol derived macromolecule **40** (Fig. 24), has shed further light on solvent-induced structural collapse. The effects of aqueous media on the conformational and chiroptical properties of these dendritic molecules (G_1 to G_3) have been studied in detail, and the importance of the hydrophobic effect in increasing structural rigidity has been highlighted.[35,36] The ORD measurements of

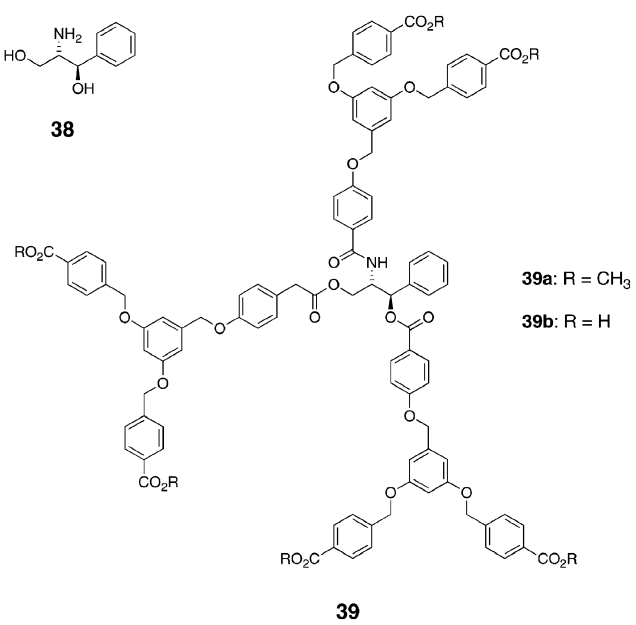

Fig. 23 Increasing steric congestion with higher generations in chiral dendrimers.

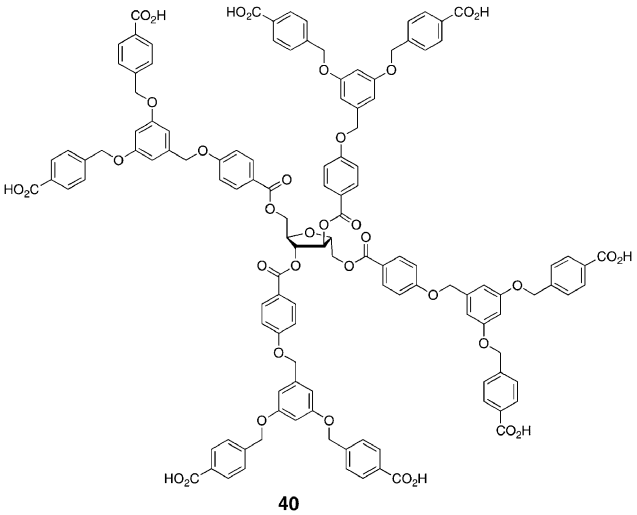

Fig. 24 First-generation chiral amphiphilic dendrimer containing a (D)-mannitol derived core and flexible polyarylether branches.

acid-terminated dendrimers **39b** and **40** in aqueous buffer indicated that both series of dendrimers exhibited rotations that varied in sign and magnitude as a function of generation. For example the absolute value of the molar rotation at 365 nm of the (D)-mannitol derived system **40** varied as follows: $G_1 = +2100$, $G_2 = -500$, $G_3 = -900$, whereas for dendrimer **39b** the absolute [ϕ] values were +400 for G_1, −475 for G_2, and +900 for G_3. The authors suggested that this observation, in conjunction with the line broadening observed in the ^{1}H NMR spectra of the dendrimers, could be rationalised by invoking internal aggregation of the macromolecules in water. Since several different equilibrating intramolecular aggregation states could be present simultaneously, this effect would contribute significantly to the unusual optical rotatory behaviour that was observed. Low intensity signals or no Cotton effect was recorded in the CD spectra for both dendrimer series in aqueous medium. In addition the CD curve was sensitive to temperature, reaching its maximum at −3 °C and then decreasing smoothly to 77 °C. The authors concluded that the variation in optical rotation data and the low intensity CD spectra of both dendrimer series **39b** and **40** in water were a result of solvent induced structural collapse, which increased the effective steric bulk of the dendritic wedges. Importantly, the associated increase in structural rigidity did not, however, create stable chiral substructures in the achiral dendritic branches as verified by CD data.

Towards total control of the creation and manipulation of chiral secondary structure

In recent years some spectacular developments have been made at the interface of synthetic and analytical chemistry in the attempt to fully comprehend and control the relationship between chiral elements and secondary structure in dendrimers. A wide range of analytical and computational techniques have been used to assist the creation of sophisticated dendritic systems. Several cases that illustrate the current level of control achievable are described in this section. In contrast to previous examples discussed in this review, the systems

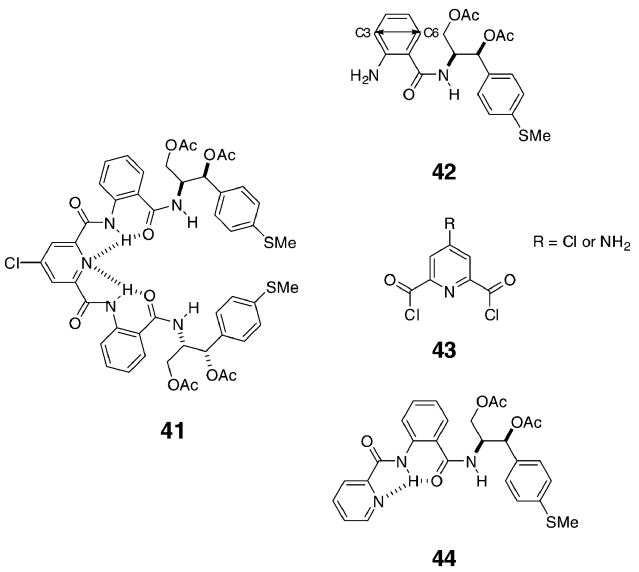

Fig. 25 First-generation chiral dendron **41**, its constituent parts **42** + **43**, and a model compound **44**.

described in this section have units built into them that readily partake in strong secondary bond formation such as hydrogen bonding.

In an attempt to create and control helical conformational stability in chiral dendrimers, Parquette examined the solvent-, temperature- and generation-dependence of intramolecularly hydrogen bonded dendrons that contained an internal anthranilamide turn unit, as exemplified by the G_1 dendron **41** (Fig. 25) prepared by attaching chiral terminus **42** to pyridine unit **43**.[37,38] ORD spectra (normalised for concentration and number of chiral termini) revealed a non-linear behaviour of magnitude and sign of rotation on going from the zeroth to third generation, indicating that a chiral secondary structure of a helical nature was developing in the dendrons. To study this further, CD spectroscopy of the first-generation dendron **41**, as well as G_2 and G_3 were compared to that of a control

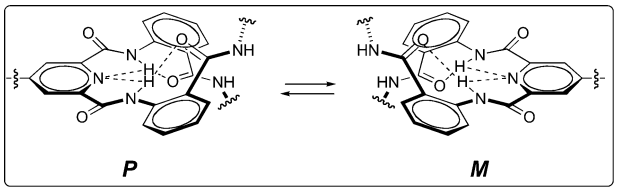

Fig. 26 Dynamic conformational equilibrium between two helical antipodes.

compound **44**, which is incapable of developing a helical secondary structure. The absolute sense of helical chirality between each pair of anthranilamide chromophores in **41** could be deduced from the shape of the curve in the 280–360 nm region of the spectrum, the band associated with the $\pi \rightarrow \pi^*$ transition along the C3–C6 axis of the anthranilamide ring. As the spectra of both compound **44** and the G_1 dendron **41** were insensitive to changes in solvent and temperatures, the authors concluded that the chiral termini **42** had "little or no influence on the position of the conformational equilibrium interconverting the two helical isomers". On comparison of **41** with the higher-generation dendrons (G_2 and G_3), the CD revealed a significant difference in the 280–360 nm region of the spectrum, indicating a change in the helical conformation (Fig. 26). In higher generations, the conformational equilibrium began to bias a single helical conformation at the periphery of the dendron and became maximal at low temperatures (−20 °C) and in poor solvents, notably 2 : 1 hexane–DCM, which enhanced the non-bonded repulsions. The authors concluded that these observations demonstrated an increase in the preference for *M* helical conformation with increasing generation and a clear dependence on both temperature and solvent. Moreover, they hinted at aggregation and compaction as potential contributing factors to the conformational bias (*vide infra*).

Later Parquette and co-workers studied the interplay between local and global compaction and how it affected the local secondary structure of folded chiral dendrimers.[39] The aim of this study was to increase the understanding of

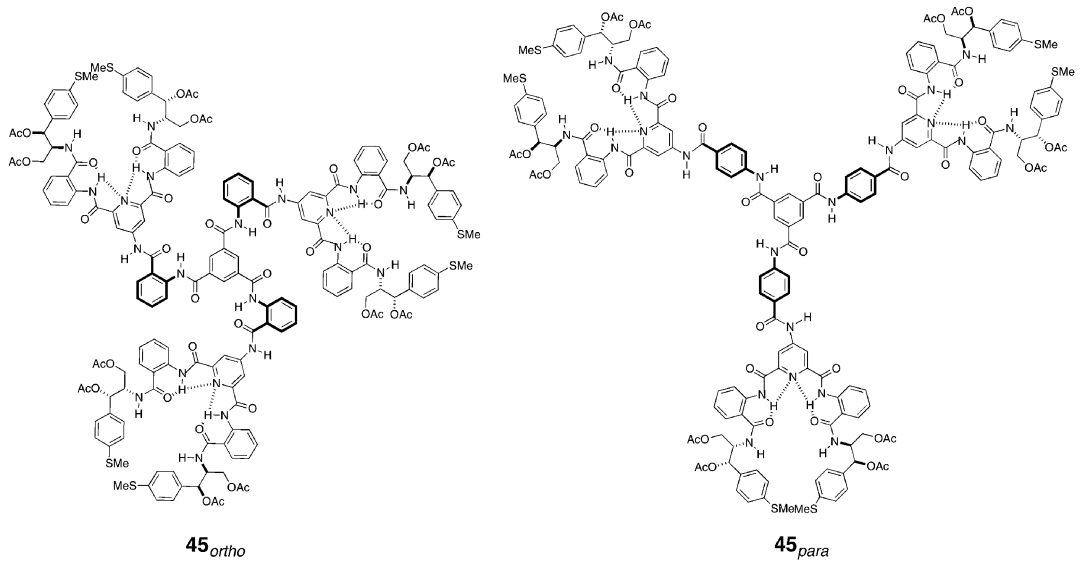

Fig. 27 First-generation *ortho*- and *para*-linked dendrimers with helically folded dendrons.

the nature of compaction in this dendritic system in order to ultimately be able to control the overall three-dimensional organisation of chiral dendrimers. Helically folded dendrons, exemplified by structure **41**, were attached *via* either a 2- or a 4-amidobenzamide linkage (*ortho*- or *para*-linkage) to a 1,3,5-benzenetricarbonyl chloride core to give two series of dendrimers G_1 to G_3, illustrated by G_1 $\mathbf{45}_{ortho}$ and $\mathbf{45}_{para}$ (Fig. 27). It was proposed that the compaction levels of the dendrimers could be adjusted by using either the *ortho*- or *para*-linkage, which would induce compacted or expanded conformations respectively. The molecular dimensions of the dendrimers were estimated through time-resolved fluorescence anisotropy (TRFA) studies. From the data collected in this study the hydrodynamic volumes (V_h) were obtained. The measured V_h was compared to the calculated van der Waals volume V_{vw}, where lower V_h/V_{vw} ratios indicated tighter packing. In general, it was noted that all *ortho*-linked dendrimers exhibited significantly higher packing efficiencies ($0.81 < V_h/V_{vw} < 1.68$) than their *para*-linked counterparts ($1.55 < V_h/V_{vw} < 6.30$). A greater solvent sensitivity was revealed for the latter system. The first-generation *ortho*-linked dendrimer $\mathbf{45}_{ortho}$ maintained a significantly more compact global structure compared for its *para*-linked analogue $\mathbf{45}_{para}$, as suggested by V_h/V_{vw}. (Solvent sensitivity of V_h was also lower for the former dendrimer) Both $\mathbf{45}_{ortho}$ and $\mathbf{45}_{para}$ exhibited a strong, negative excitonic couplet at 316 nm in the CD spectrum, consistent with a shift in the conformational equilibrium toward *M* helical conformation (see Fig. 26), but this was highly sensitive to increasing temperatures in MeCN solution. Notably, on addition of 10% EtOH to a DCM solution, both $\mathbf{45}_{ortho}$ and $\mathbf{45}_{para}$ expanded slightly, whereas on addition of 50% EtOH the intramolecular hydrogen bonds became severely disrupted, leading to a dramatic structural collapse. The authors concluded that the correlation of low V_h/V_{vw} values with an increase in the stability of the helical bias indicated that compaction of the dendritic structure was important for stabilising the secondary structural features of the dendrimers. CD studies for the G_2 dendrimers also indicated a greater bias for the *M* helical conformation, in addition to a substantial temperature and solvent dependence. It was not possible to determine the V_h for the G_3 dendrimers, although the authors suggested that the trend of increasing level of compaction was likely to increase further from G_2 to G_3. Surprisingly, the CD of the *ortho*-linked G_3 dendrimer exhibited a positive excitonic couplet, indicating a bias towards *P* helical conformation, in contrast to the preference for *M* helices observed for all other dendrimers. The authors could not fully rationalise this change in preference but suggested that it was ''consistent with the general trend observed beginning at the second generation for the nonlocal interactions to oppose the secondary structural preference of the isolated dendrons''.

Building on previous attempts to control the bias of helical conformation of chiral intramolecularly hydrogen bonded dendrons, Parquette and co-workers demonstrated how the conformations of the dendrons could be 'locked' by coordination to copper(II) metal centres, as illustrated by the G_2 metallodendron **46** (Fig. 28).[40] The CD spectrum of the first-generation dendron complexed to copper(II) indicated that the anthranilamide terminal groups adopted an *M* chiral helical

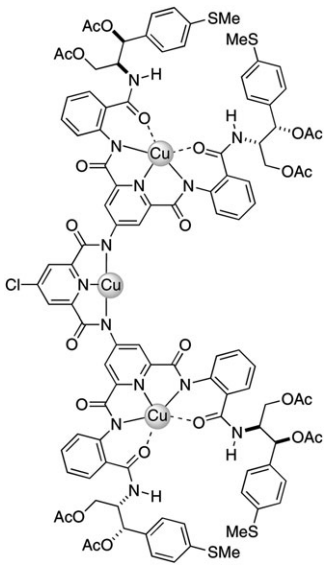

46

Fig. 28 A second-generation dendron in which the *M* helical conformation is locked by coordination to copper(II).

conformation, which was unbiased prior to metal coordination. (Note that the G_2 and G_3 dendrons *did* exhibit an *M* helical bias prior to coordination to copper) Moreover, the CD spectra of the copper-complexed G_1 dendron was stable to temperatures up to 60 °C in MeCN [110 °C in bis(2-butoxyethyl)ether]. As each pyridine-2,6-dicarboxamide repeat unit in the dendrons is covalently bonded to a metal centre this forces the subunit to exist in a *syn–syn* (lowest energy) conformation exclusively, as depicted in Scheme 2. Consequently the *M* helical conformation was dramatically rigidified in the dendron structure by coordination to a copper metal centre.

Drawing on early studies of metallodendrons, the same group developed a modified dendritic system, which contained chiral oxazolines on the dendron termini coupled to the pyridyl units **43** (Fig. 25). Due to the differing coordination properties of oxazolines and pyridines, unique metals such as Cu and Ni could be installed at the focal and peripheral shells of the dendron respectively, as shown in structure **47** (Fig. 29).[41] CD spectroscopy revealed that a rigid *P* helical conformation was maintained upon metal coordination.

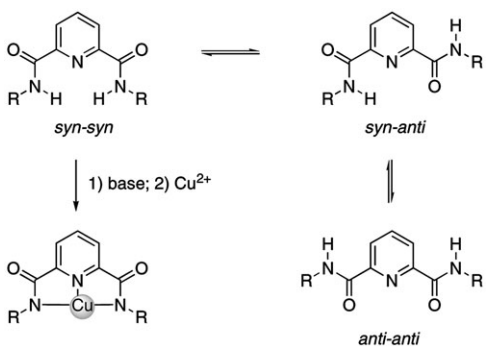

Scheme 2 Conformational locking of pyridine-2,6-dicarboxamide by copper(II).

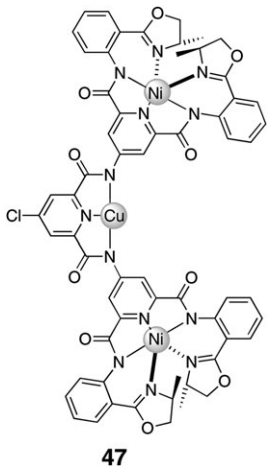

47

Fig. 29 Shell-selective metalation of oxazoline-terminated dendrons.

Furthermore the amplitude of the CD signals of the metallo-dendron showed no temperature sensitivity up to 60 °C unlike the parent (uncomplexed) dendron.

A study of dendron folding in water was carried out by Hofacker and Parquette on the second-generation dendron **48** (Fig. 30) containing chiral pentaethylene glycol termini, and its G_1 and G_3 analogues.[42] Conformational analysis by CD spectroscopy revealed a spectacular solvent-mediated switch of helical chirality, in which the helical conformation of the pyridine-2,6-carboxamide repeat unit changed from *M* in THF (intense negative couplet at 316 nm) to *P* in water (intense positive couplet at 316 nm). Dilution studies over a 100-fold concentration range ruled out aggregation as a contributing factor to the $M \rightarrow P$ helical inversion. This helical transition was displayed in first- to third-generation dendrons. Interestingly, IR spectroscopy in combination with molecular dynamics simulations indicated that the solvation of dendron

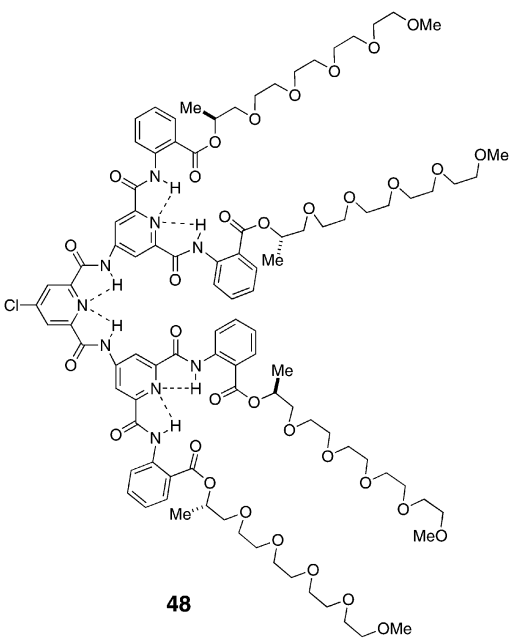

48

Fig. 30 A water-soluble G_2 dendron with chiral pentaethylene glycol termini.

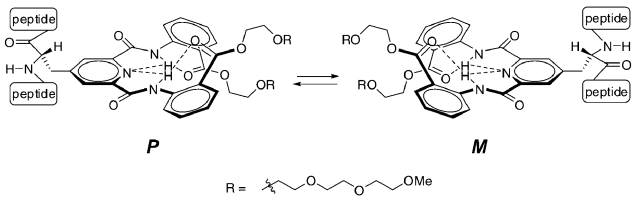

Fig. 31 Helical conformational equilibria of dendron-modified alanine residues appended to a peptide backbone.

48 in water induced a *gauche* → *anti* conformational shift about the C–O bonds in the terminal pentaethylene glycol chains, which in turn induced an inversion in the helical secondary structures within the dendron.

In a recent study by the same group, dendron-modified amino acid residues were inserted at specific positions into a peptide sequence, as illustrated by Fig. 31.[43] In view of previous results, which demonstrated a solvent-mediated inversion of helicity, the authors reasoned that an assembly that combined peptide folding with dendron packing would mediate efficient chiral communication. CD and FT-IR spectroscopy were used to measure the conformational states of the dendron and the peptide backbone independently. The helical bias in the dendrons was observed in the CD spectrum by the excitonic couplet at 316 nm (as previously), whereas the peptide conformation was studied at 218–222 nm. Two alanine-rich systems, chosen because of the tendency of alanine-dominated peptides to adopt the α-helix form, were found to adopt a β-sheet structure in aqueous buffer. On addition of trifluoroethanol, it was noted that the peptide–dendron conjugate reverted to the α-helical form. The authors concluded that the β-sheet to α-helix conformational equilibrium is governed in an inherently alanine-rich peptide sequence by intermolecular hydrophobic association of its dendritic side chains in water.

Combinatorial chemistry has been used by the Hirsch group to prepare small libraries of G_0 to G_3 depsipeptide dendrons (Fig. 32), starting from (*R*,*R*)-, (*S*,*S*)- and *meso*-tartaric acid as branching units and dipeptides or tripeptides consisting of (L)-alanine, (L)-leucine and glycine as chiral-spacer building blocks.[44] The authors noted a non-linear behaviour in both the specific and molar rotation values with increasing generation but concluded, however, that folding phenomena due to the formation of chiral secondary structures was not occuring, since (to a first approximation) the $[\phi]$ of larger dendritic systems represented the sum of their constituent building blocks.

Later, the same authors attempted to induce chiral folding in these depsipetide dendrimers containing an EDTA-derived core by complexation to copper(II) or zinc(II), as illustrated by the G_3 dendrimer in Fig. 33.[45] It was found that this class of dendrimers exhibited well-defined diastereoselective folding upon metal complexation to the EDTA core. Initial studies (CD, X-ray) of a model compound suggested preferential formation of a copper complex with *cis*-α coordination geometry. Subsequently, the CD spectra of G_1 and G_2 dendritic ligands were compared to those of their copper-complexed analogues. For the metallo-dendrimers, four distinct peaks were identified in the CD. These were centred around 310, 340,

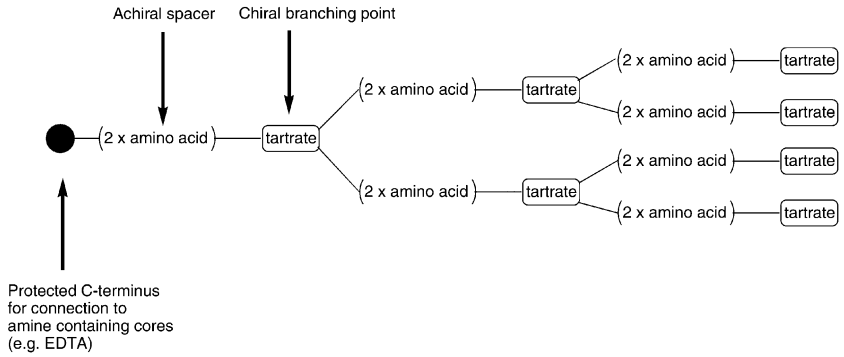

Fig. 32 A third-generation chiral depsipeptide dendron.

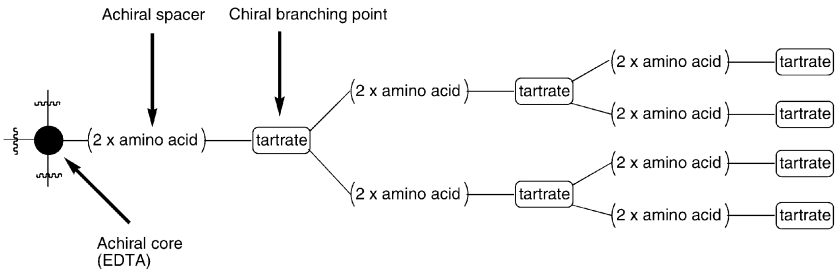

Fig. 33 A third-generation chiral depsipeptide dendrimer containing an achiral EDTA-derived core.

380 and 700 nm (the uncomplexed dendrimers did not exhibit any CD activity at these wavelengths). The authors proposed that the CD spectra were ''indicative of chirality transfer from the ligand to the metal, which as a result of stereoselectivity, leads to the preferred formation of a chiral conformation motif''. Notably, the G_1- and G_2-metallodendrimers exhibited opposite signs in their CD curves. Moreover, the G_1 copper-complexed dendrimer adopted a Λ*cis*-α(*R*,*R*) whereas its G_2 analogue adopted the opposite configuration [Δ*cis*-α(*S*,*S*)] (see Fig. 34), in which (*R*,*R*) and (*S*,*S*) refer to the chirality of the EDTA nitrogens. Assignment of the absolute configuration was performed by comparison to calculated CD spectra (of the optimised structures). Thus the authors concluded that they had achieved a metal-complexation-induced diastereoselective folding in chiral dendrimers, although at the time they were unable to understand why the two dendrimers, which differed in the steric demand of the dendritic branches, would favour different configurations.

Much recent attention has been devoted to the study of dendrimer-based supramolecular host–guest complexes in order to develop suitable dendritic systems where a chiral secondary structure could be induced onto an achiral core from chiral branches *via* intermolecular electrostatic or hydrogen bonding. Meijer and co-workers conducted NMR and chiroptical studies of host–guest complexes of increasing generations (G_1 to G_5), in which the host structure was a urea–adamantyl terminated poly(propylene imine) dendrimer, and the guest molecule a ureido–acetic acid derivative with a chiral amino acid terminus, as illustrated by the supramolecular dendritic structure in Fig. 35.[46] ^{1}H–^{1}H NOESY spectroscopy confirmed the existence of a supramolecular structure, and the measurement of T_1 relaxation times indicated that the dendrimer periphery became more rigid when guest molecules were bound to the dendritic host through complexation. Optical rotation measurements showed a constant value for [α] for the complexes of different generations of the urea–adamantyl dendrimer and *N*-Boc-(L)-phenylalanine terminated guest molecules (non-covalently attached), which suggested that the local conformational freedom of the amino acid termini remained constant despite the increasing size and

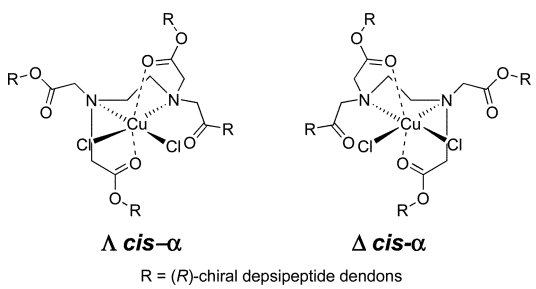

Fig. 34 Configuration of EDTA backbone.

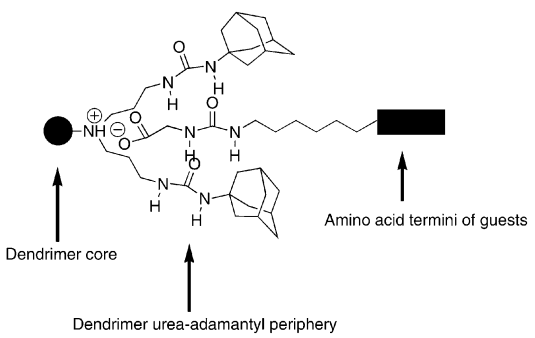

Fig. 35 A chiral dendritic host–guest system.

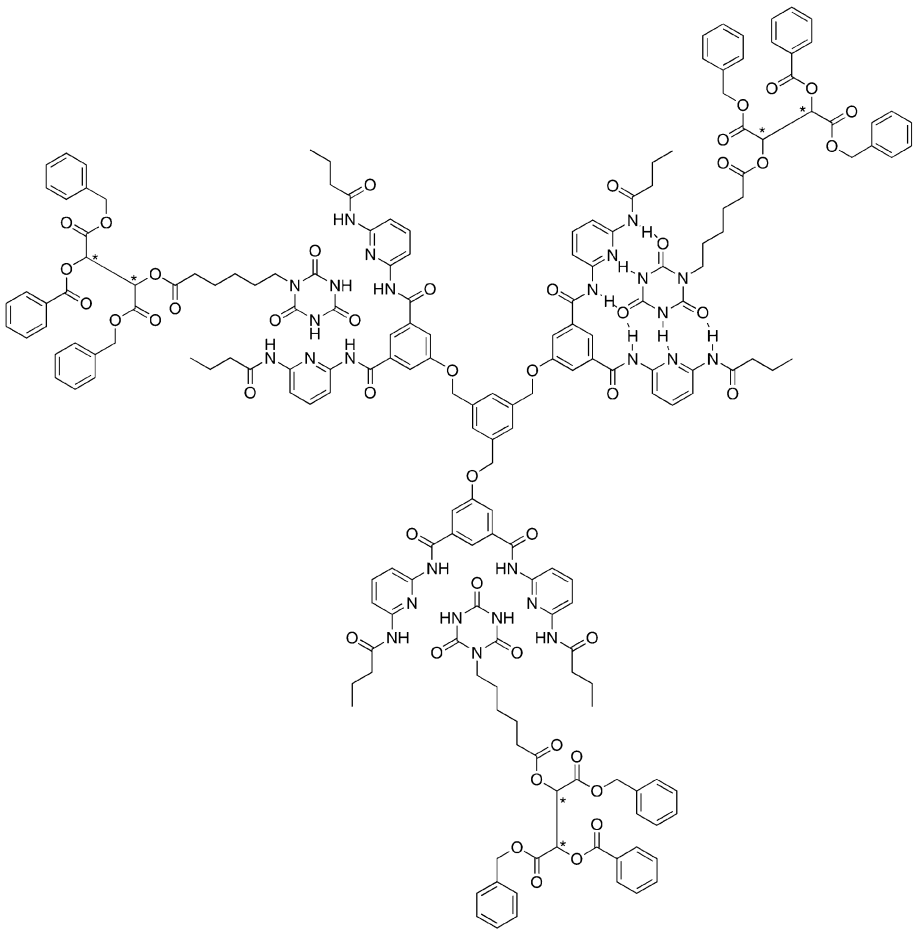

49

Fig. 36 A first-generation self-assembled chiral depsipeptide dendrimer.

overall rigidity of the macromolecule. The authors concluded that these (seemingly contradictive) observations indicated that the guest molecules constantly associate and disassociate from the dendrimer.

Hirsch and co-workers demonstrated a high level of control in the self-assembly of chiral depsipeptide dendrimers,[47,48] exemplified by the first-generation macromolecule **49** (Fig. 36), consisting of an achiral homotritopic Hamilton receptor (core) and cyanurate-terminated chiral depsipeptide branches attached to the receptor through complementary hydrogen bonding motifs.[47] The binding cooperativity of this class of supramolecular dendrimers (G_1 to G_3) was assessed by NMR titration studies. Statistical analysis of the ^{1}H NMR titration plots and associated calculations indicated that the binding cooperativity for both G_1 and G_2 dendrons was much higher than that for the G_3 analogues. The authors reasoned that the binding of two G_1 and G_2 dendrons would introduce additional sterical constraints and thus force the remaining Hamilton receptor binding site to a preference for the *cis–cis* conformation. This particular conformation would, in turn, have the highest susceptibility for the binding of another cyanurate dendron, due to its favourable preorganisation. As the steric demand was greater, this effect was more pronounced in the G_2 than in the G_1 systems. In the G_3 dendrons,

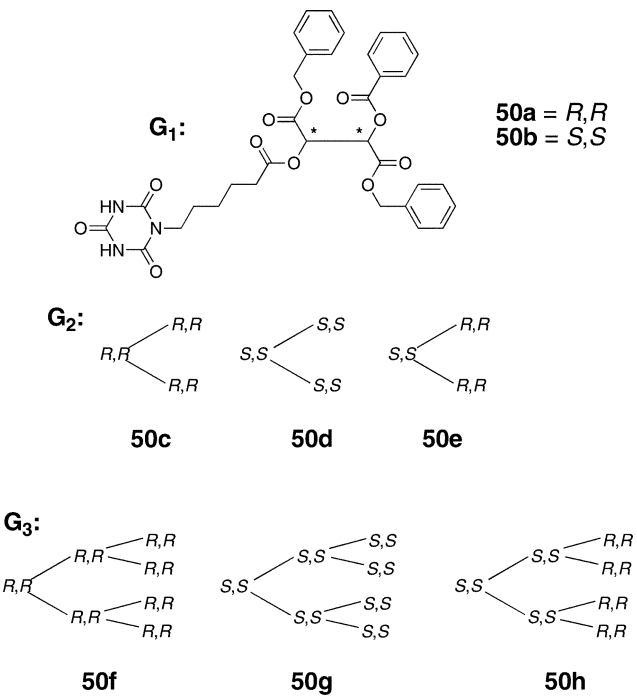

Fig. 37 Chiral layers in first- to third-generation depsipeptide dendrons.

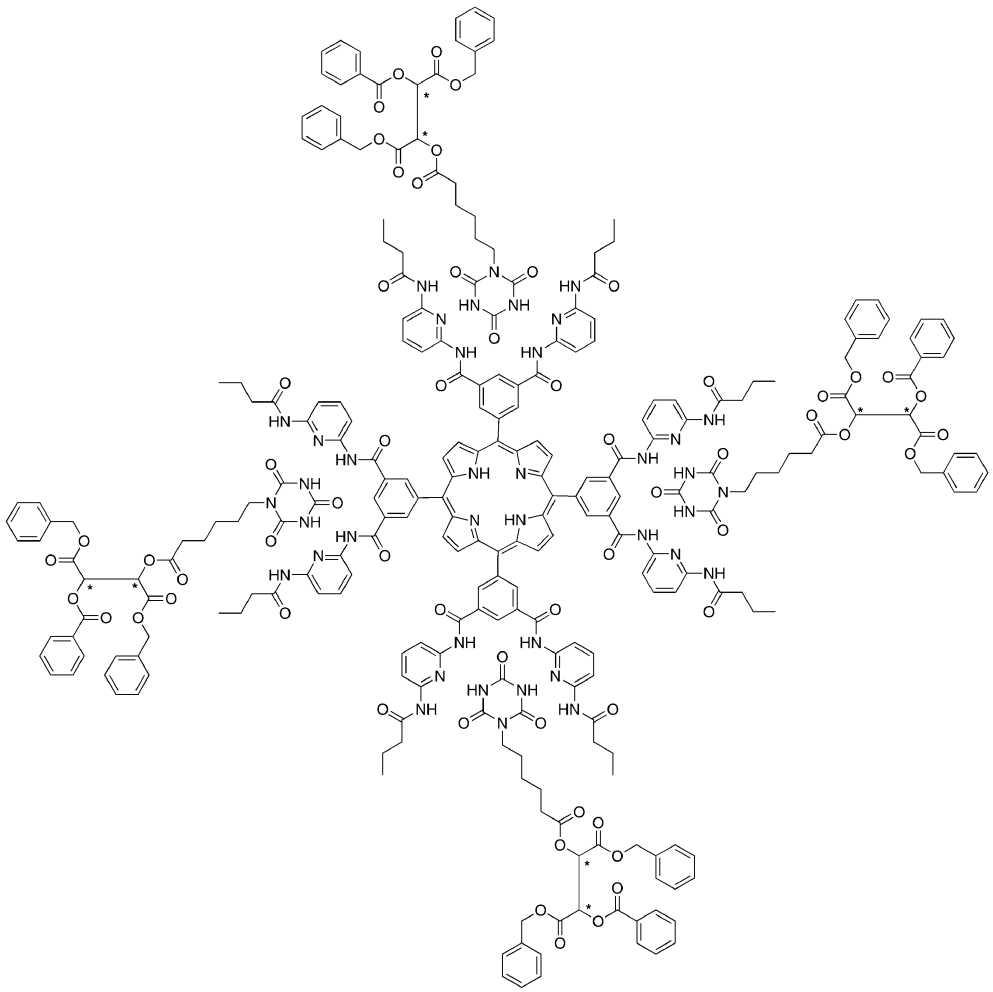

51

Fig. 38 A first-generation chiral depsipeptide dendrimer with a porphyrin-based core.

however, the dendritic ligands are so bulky that their threefold binding mode becomes less favourable again. CD spectroscopy of **49** and its G_2 and G_3 analogues revealed a characteristic absorption band at 310 nm, indicative of a chirality transfer from the chiral dendrons (Fig. 37) to the achiral Hamilton receptor. This signal was distinct from the absorption of the aromatic groups of the chiral dendrons **50** at about 250 nm. Interestingly, a distinct diastereoselectivity was observed for the binding cooperativities for the second-generation depsipeptide dendrons. A substantially higher binding cooperativity was noted for the heterochiral dendron **50e** compared for the binding of the homochiral analogues **50c** and **50d**. However, observation that the CD curves of the diastereoisomeric complexes (*e.g.* involving guests **50d/50e**, or **50g/50h**) had the same characteristic shape led the authors to conclude that the chiroptical properties were due to ''statistical chirality transfer from the chiral dendrons only'', and *not* resulting from diastereoselective formation of chiral foldamers.

A similar study was later conducted on a porphyrin-based analogue, exemplified by the first-generation dendrimer **51** in Fig. 38.[48] The porphyrin core was chosen for chiroptical studies due to it having clearly separated electronic absorptions (λ_{max} at 302 and 420 nm). Chirality transfer from the depsipeptide branches to the achiral porphyrin core was probed by CD spectroscopy, and found to occur for the second- and third-generation dendritic assemblies, but not the first generation. The four fold binding to the porphyrin receptor proved more effective for the G_2 dendrons than for their bulkier G_3 analogues. It was assumed that the most stable conformation of a complex such as **51** should have a chiral propeller-like shape with two enantiomeric right- or left-handed conformations. This assumption was based on examination of X-ray crystal structures of a series of *meso*-aryl-substituted porphyrins, which showed that the aryl rings were in most cases not oriented perpendicularly to the porphyrin plane but exhibited typical angles in the range between 65 and 80°.

Finally, in a different study of host–guest chemistry and chirality transfer in dendritic structures directed towards sensor design, Aida and co-workers elegantly evaluated

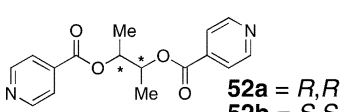

52a = *R,R*
52b = *S,S*

52

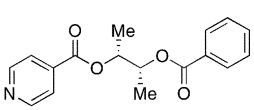

53

Fig. 39 Chiral guest molecules.

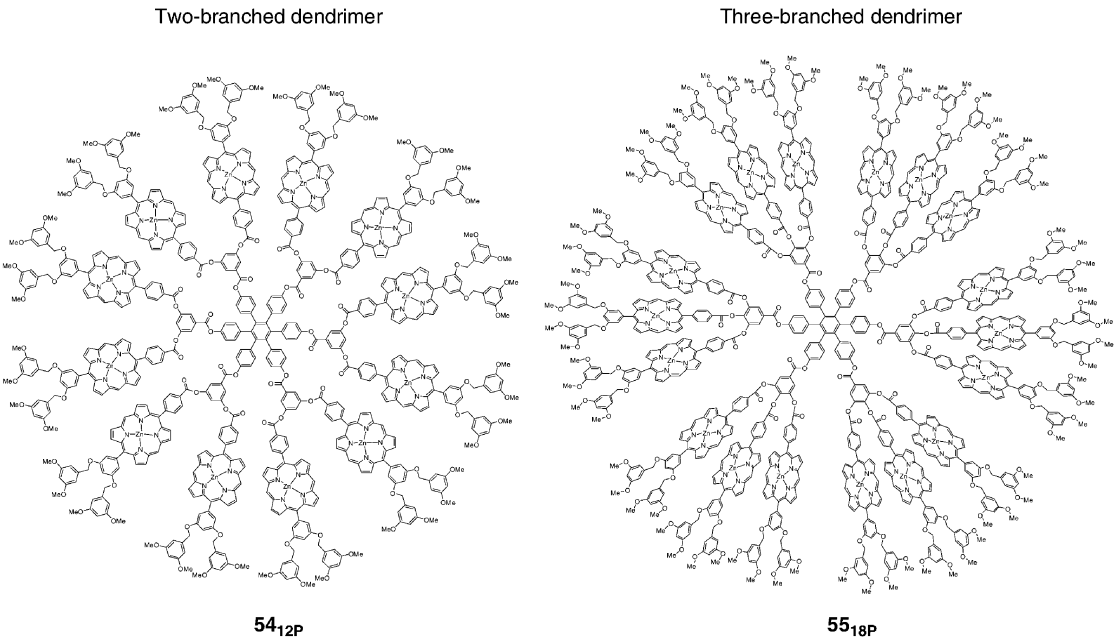

Fig. 40 Achiral zinc–porphyrin appended two- and three-branched dendritic hosts.

whether chiral bidentate guest molecules **52a–b** or the monodentate analogue **53** (Fig. 39) could induce chiral conformations in Zn–porphyrin based dendrimer hosts of first to third generation.[49] The two classes of achiral dendritic hosts studied were the doubly and triply branched macromolecules, which carry 12 and 18 porphyrin units respectively, illustrated by $\mathbf{54_{12P}}$ and $\mathbf{55_{18P}}$ in Fig. 40. Higher generation doubly and triply branched dendrimers bearing 24 and 36 porphyrin units, respectively ($\mathbf{54_{24P}}$ and $\mathbf{55_{36P}}$, not depicted) were also synthesised. Their potential use as chiroptical sensors was evaluated with CD spectroscopy. The enantiomers of the bidentate guest molecules (**52a** and **52b**) induced distinctive s-shaped signals in the 400–450 nm region on ligation to the dendritic host $\mathbf{54_{24P}}$. (In contrast the monodentate guest molecule **53** induced no chiroptical response) The maximum CD amplitudes in the same spectral region were found to increase with dendrimer size for both the two- and three-branched dendrimer systems. When these values were divided by the amount of zinc porphyrin units, and compared to the association constants of the dendritic hosts, the authors could identify the optimum structure for chiral recognition. It was concluded that the two-branched system **54** constituted a more suitable chiroptical sensor for the recognition of guest molecules **52a** and **52b**, and that a ''cooperative function of multiple zinc porphyrin units on the dendrimer scaffold [could be used] for efficient translation of chiral information''. The authors also proposed that the large chiroptical response in the CD of $\mathbf{54_{24P}}$ could originate from a twisted geometry of the guest-binding zinc porphyrins on the dendrimer scaffold.

Conclusions

To dictate the overall chiral conformational order of dendritic structures by manipulation of individual chiral elements has proven to be a considerable challenge. Beautiful and sometimes highly sophisticated dendrimers have been studied in recent years, and several important issues have been highlighted that underscore the many predicaments associated with detecting the creation of a chiral secondary structure in these fascinating macromolecules. In recent years the understanding and manipulation of these systems has really begun to flourish as a result of the creative combination of increasingly sophisticated synthetic, analytical and computational techniques. The levels of control now achievable suggest that an extensive range of novel applications of chiral designer dendrimers will be available in the near future.

Acknowledgements

The authors thank Novartis UK Ltd, for generous studentship support (to J. T. R.).

References

1 C. J. Hawker and K. L. Wooley, *Science*, 2005, **309**, 1200–1205.
2 T. Darbre and J.-L. Reymond, *Acc. Chem. Res.*, 2006, **39**, 925–934.
3 X. Hu, Q. An, G. Li, S. Tao and J. Liu, *Angew. Chem., Int. Ed.*, 2006, **45**, 8145–8148.
4 C.-S. Ha and J. A. Gardella, *Chem. Rev.*, 2005, **105**, 4205–4232.
5 A. Lendlein, H. Jiang, O. Jünger and R. Langer, *Nature*, 2005, **434**, 879–882.
6 R. Malik, R. Duncan, D. A. Tomalia and R. Esfand, *US Pat.*, 7 005 124, 2006.
7 For an excellent discussion of chiral dendrimers and their applications in asymmetric catalysis, see: B. Romagnoli and W. Hayes, *J. Mater. Chem.*, 2002, 767–799.
8 U. Hahn, A. Kaufmann, M. Nieger, O. Julinek, M. Urbanova and F. Vögtle, *Eur. J. Org. Chem.*, 2006, 1237–1244.
9 B. Romagnoli, I. van Baal, D. W. Price, L. M. Harwood and W. Hayes, *Eur. J. Org. Chem.*, 2004, 4148–4157.
10 H. W. I. Peerlings, M. P. Struijk and E. W. Meijer, *Chirality*, 1998, **10**, 46–52.
11 H. W. I. Peerlings, D. C. Trimbach and E. W. Meijer, *Chem. Commun.*, 1998, 497–498.

12 P. Murer and D. Seebach, *Angew. Chem., Int. Ed. Engl.*, 1995, **34**, 2116–2119.
13 P. Murer, D. Seebach, J.-M. Lapierre and G. Greiveldinger, *Helv. Chim. Acta*, 1997, **80**, 1648–1681.
14 H.-F. Chow and C. C. Mak, *J. Chem. Soc., Perkin Trans. 1*, 1994, 2223–2228.
15 H.-F. Chow, L. F. Fok and C. C. Mak, *Tetrahedron Lett.*, 1994, **35**, 3547–3550.
16 H.-F. Chow and C. C. Mak, *Pure Appl. Chem.*, 1997, **69**, 483–488.
17 H.-F. Chow and C. C. Mak, *J. Chem. Soc., Perkin Trans. 1*, 1997, 91–95.
18 A. R. E. Brewer, A. F. Drake, S. E. Gibson and J. T. Rendell, *Org. Lett.*, 2007, **9**, 3487–3490.
19 V. Lellek and I. Stibor, *J. Mater. Chem.*, 2000, **10**, 1061–1073.
20 J. F. G. A. Jansen, H. W. I. Peerlings, E. M. M. de Brabander-van den Berg and E. W. Meijer, *Angew. Chem., Int. Ed. Engl.*, 1995, **34**, 1206–1209.
21 H. Zhao, F. Sanda and T. Masuda, *Macromol. Chem. Phys.*, 2006, **207**, 1921–1926.
22 C. O. Turrin, J. Chiffre, D. de Montauzon, G. Balavoine, E. Manoury, A. M. Caminade and J. P. Majoral, *Organometallics*, 2002, **21**, 1891–1897.
23 C. Reuter, G. Pawlitzki, U. Wörsdörfer, M. Plevoets, A. Mohry, T. Kubota, Y. Okamoto and F. Vögtle, *Eur. J. Org. Chem.*, 2000, 3059–3067.
24 Y.-M. Chen, C.-F. Chen and F. Xi, *Chirality*, 1998, **10**, 661–666.
25 H. W. I. Peerlings and E. W. Meijer, *Eur. J. Org. Chem.*, 1998, 573–577.
26 C. Rosini, S. Superchi, H. W. I. Peerlings and E. W. Meijer, *Eur. J. Org. Chem.*, 2000, 61–71.
27 L. Ma, S. J. Lee and W. Lin, *Macromolecules*, 2002, **35**, 6178–6184.
28 Q. S. Hu, V. Pugh, M. Sabat and L. Pu, *J. Org. Chem.*, 1999, **64**, 7528–7536.
29 L. Pu, *Macromol. Rapid Commun.*, 2000, **21**, 795–809.
30 A. Ritzén and T. Frejd, *Eur. J. Org. Chem.*, 2000, 3771–3782.
31 J. R. McElhanon and D. V. McGrath, *J. Am. Chem. Soc.*, 1998, **120**, 1647–1656.
32 J. R. McElhanon and D. V. McGrath, *J. Org. Chem.*, 2000, **65**, 3525–3529.
33 D. M. Junge and D. V. McGrath, *Tetrahedron Lett.*, 1998, **39**, 1701–1704.
34 J. L. Chaumette, M. J. Laufersweiler and J. R. Parquette, *J. Org. Chem.*, 1998, **63**, 9399–9405.
35 M. J. Laufersweiler, J. M. Rohde, J. L. Chaumette, D. Sarazin and J. R. Parquette, *J. Org. Chem.*, 2001, **66**, 6440–6452.
36 J. G. Weintraub, S. Broxer, N. M. Paul and J. R. Parquette, *Tetrahedron*, 2001, **57**, 9393–9402.
37 J. Recker, D. J. Tomcik and J. R. Parquette, *J. Am. Chem. Soc.*, 2000, **122**, 10298–10307.
38 B. Huang and J. R. Parquette, *J. Am. Chem. Soc.*, 2001, **123**, 2689–2690.
39 B. Huang, M. A. Prantil, T. L. Gustafson and J. R. Parquette, *J. Am. Chem. Soc.*, 2003, **125**, 14518–14530.
40 M. R. Rauckhorst, P. J. Wilson, S. A. Hatcher, C. M. Hadad and J. R. Parquette, *Tetrahedron*, 2003, **59**, 3917–3923.
41 A. J. Preston, J. C. Gallucci and J. R. Parquette, *Org. Lett.*, 2006, **8**, 5885–5888.
42 A. L. Hofacker and J. R. Parquette, *Angew. Chem., Int. Ed.*, 2005, **44**, 1053–1057.
43 H. Shao, J. W. Lockman and J. R. Parquette, *J. Am. Chem. Soc.*, 2007, **129**, 1884–1885.
44 J. Kress, A. Rosner and A. Hirsch, *Chem.–Eur. J.*, 2000, **6**, 247–257.
45 B. Buschhaus, F. Hampel, S. Grimme and A. Hirsch, *Chem.–Eur. J.*, 2005, **11**, 3530–3540.
46 M. A. C. Broeren, B. F. M. de Waal, J. L. J. van Dongen, M. H. P. van Genderen and E. W. Meijer, *Org. Biomol. Chem.*, 2005, **3**, 281–285.
47 K. Hager, A. Franz and A. Hirsch, *Chem.–Eur. J.*, 2006, **12**, 2663–2679.
48 K. Maurer, K. Hager and A. Hirsch, *Eur. J. Org. Chem.*, 2006, 3338–3347.
49 W. S. Li, D. L. Jiang, Y. Suna and T. Aida, *J. Am. Chem. Soc.*, 2005, **127**, 7700–7702.